# Spanning connectivity in a multilayer network and its relationship to site-bond percolation

Saikat Guha, Donald Towsley, Philippe Nain, Cagatay Capar, Ananthram Swami, Prithwish Basu

# Spanning connectivity in a multilayer network and its relationship to site-bond percolation

Saikat Guha,[1] Donald Towsley,[2] Philippe Nain,[3] Çağatay Çapar,[4] Ananthram Swami,[5] and Prithwish Basu[1]
[1]*Raytheon BBN Technologies, Cambridge, Massachusetts 02138, USA*
[2]*University of Massachusetts, Amherst, Massachusetts 01003, USA*
[3]*Inria, 06902 Sophia Antipolis Cedex, France*
[4]*Ericsson Research, San Jose, California 95134, USA*
[5]*US Army Research Laboratory, Adelphi, Maryland 20783, USA*
(Received 6 October 2015; revised manuscript received 3 March 2016; published 14 June 2016)

We analyze the connectivity of an $M$-layer network over a common set of nodes that are active only in a fraction of the layers. Each layer is assumed to be a subgraph (of an underlying connectivity graph $G$) induced by each node being active in any given layer with probability $q$. The $M$-layer network is formed by aggregating the edges over all $M$ layers. We show that when $q$ exceeds a threshold $q_c(M)$, a giant connected component appears in the $M$-layer network—thereby enabling far-away users to connect using "bridge" nodes that are active in multiple network layers—even though the individual layers may only have small disconnected islands of connectivity. We show that $q_c(M) \lesssim \sqrt{-\ln(1-p_c)}/\sqrt{M}$, where $p_c$ is the bond percolation threshold of $G$, and $q_c(1) \equiv q_c$ is its site-percolation threshold. We find $q_c(M)$ exactly for when $G$ is a large random network with an arbitrary node-degree distribution. We find $q_c(M)$ numerically for various regular lattices and find an exact lower bound for the kagome lattice. Finally, we find an intriguingly close connection between this multilayer percolation model and the well-studied problem of site-bond percolation in the sense that both models provide a smooth transition between the traditional site- and bond-percolation models. Using this connection, we translate known analytical approximations of the site-bond critical region, which are functions only of $p_c$ and $q_c$ of the respective lattice, to excellent general approximations of the multilayer connectivity threshold $q_c(M)$.

DOI: 10.1103/PhysRevE.93.062310

## I. INTRODUCTION

Since the mid-2000s there has been a surge of interest in multilayer networks, several properties of various genres that have been studied. Much of this recent work has been covered in these two review articles [1,2]. Specific example studies include the diffusion dynamics of multilayer networks [3], cascades [4,5], spectral properties [6], robustness analysis stemming from overlapping multilayer links [7], growing random multilayer networks [8], epidemic spread [9], a tensorial formulation [10], and algorithmic complexity of finding short paths through co-evolving multilayer networks [11]. The connectivity properties of random multilayer networks have also been studied, such as the study of the properties of the giant connected component (GCC) in a random network with correlated multiplexicity, i.e., where the node degree distributions across layers have positive (or negative) correlations [12].

The multilayer network model we study in this paper was inspired by a multichannel wireless *ad hoc* communication network [13], where each node only uses a small subset of all the available channels at any given time (to save energy—battery life of a radio transceiver, for instance), and the consideration of the minimum number of channels in which each node should be active to ensure long range connectivity.

We consider a set of users connected via $M$ coexisting networks $G_1, \ldots, G_M$. Let us assume that each user (node) is active only in a subset of these networks. Consequently, a user who is active in both $G_1$ and $G_2$ can help connect two other users that are active in $G_1$ alone, and in $G_2$ alone, respectively, by forming a bridge. Figure 1 illustrates an example with $M = 3$ networks ("layers"), where a path connecting $v_1$ and $v_2$ must traverse all three layers, and one such path is shown to go through the bridge nodes $v_3$ and $v_4$, both of which are occupied in more than one layer.

Some concrete examples of such multilayer networks are (1) a network of cities connected via different airline companies where each city is served only by a subset of all the airlines [11,14], (2) a network of users with accounts on multiple online social networks [15], and (3) a military communication network of units equipped with radios that can listen and transmit simultaneously on a subset of multiple frequencies [13]. Each of these scenarios have one feature in common: The multilayer network is formed over a *common* set of nodes via coexisting means of connectivity. In other words, each node in the multilayer network is one single entity (e.g., a city, a social network user, or a multichannel radio) that may be active simultaneously in a subset of multiple layers, where each layer that a given node is active in, provides a distinct mode for that node to connect to its neighboring nodes that are also active in that layer.

In our analysis in this paper, we will make a simplifying assumption that each network layer is a subgraph of a *common* underlying connectivity graph $G(V,E)$ whose edge set $E$ defines all the *possible* connections, some of which may be dormant if the two nodes an edge connects are not active in at least one common layer. The underlying connectivity graphs for the aforesaid examples are the network of airway passages connecting the cities, the underlying friendship network (who is a friend of whom on social networks), and the Euclidean geometric graph induced by the locations of the multichannel radios and their maximum range, respectively.

Each node will be assumed to be active in a given layer with probability $q$, and the node occupancies in each layer will be

 

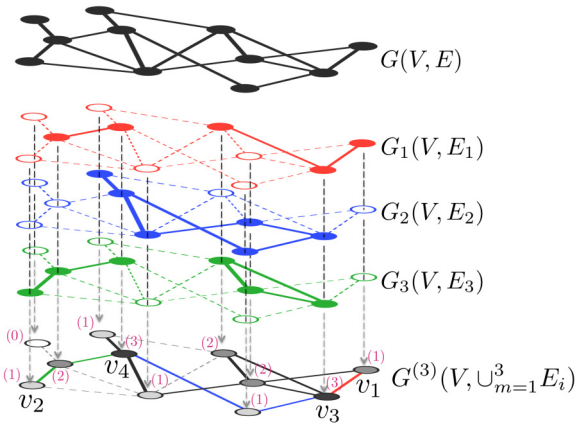


FIG. 1. Schematic of a three-layer network. The numbers of layers in which each node is occupied (active) are shown.

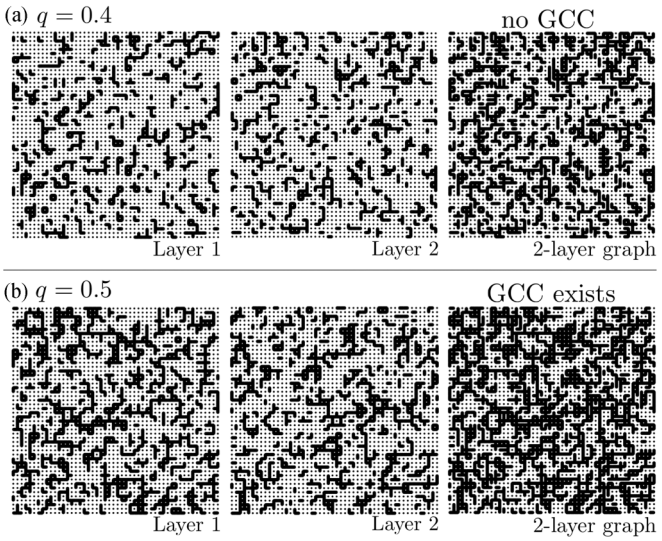


FIG. 2. Two independent site-percolation instances ("layers") of a square grid $G$ are shown for site-occupation probability (a) $q = 0.4$ and (b) $q = 0.5$. Each site in each layer is occupied with probability $q$, and a bond is activated when both sites at its end points are occupied. Active bonds are shown by black line segments. A two-layer lattice is formed by first marking as occupied all those sites in $G$ that are occupied in at least one of two independent *layers* (site-percolation instances of $G$) and then activating all the bonds that have sites at both their end points occupied. The site-percolation threshold of a square grid, $q_c \equiv q_c(1) \approx 0.59$, which is why the single layer graphs do not have a giant connected component (GCC) either for $q = 0.4$ or $q = 0.5$. However, the two-layer percolation threshold for the square lattice, $q_c(2) \approx 0.47$. Thus, the two-layer graph created with $q = 0.4$ does not exhibit a GCC, whereas the one created with $q = 0.5$ does.

taken to be independent. The subgraph corresponding to the $m$th layer $G_m(V,E_m)$ is obtained by removing all the edges of $G(V,E)$ both of whose end nodes are not active in the $m$th layer. The merged (random) graph $G^{(M)}(V,\cup_{m=1}^{M}E_m) \subset G$ represents the effective multilayer network whose edges can connect the nodes in $V$. So the $M$-layer graph $G^{(M)}$ is formed by directly aggregating the edges over all $M$ layers. For an edge to exist in $G^{(M)}$, the two nodes it connects must be active in at least one common layer. Since each node is a single physical entity, one can think of the interlayer connectivity graph at a given node to be a $k$-clique, where $k$ is the number of layers in which the node is occupied. Our goal in this paper is to study the threshold value of the single-layer node-occupation probability $q$, which we will denote $q_c(M)$, when a GCC (or a spanning cluster) appears in the $M$-layer network $G^{(M)}$, at which point distant users can connect using a series of bridge nodes that are active in multiple layers, even though the individual layers may only have small disconnected islands of connectivity. Clearly, for $M = 1$, this model reduces to the standard independent and identically distributed site-percolation problem, and thus $q_c(1) = q_c$, the site-percolation threshold of $G$. In Fig. 2, we show an illustrative numerical example for two layers over a square grid.

As the reader may already have noted, the model we analyze in this paper is insufficient to accurately model most practical multilayer networks. For instance, the assumption that each individual network layer is an induced subgraph of a common underlying graph may not be accurate. For example, in a multilayer social network, a node's neighbors (friends) in LinkedIn may differ from its neighbors in Facebook. On the other hand, in the multichannel wireless *ad hoc* network example described above, the assumption that each layer samples from one underlying connectivity graph is quite accurate. Several other interesting extensions of our model are described in the Conclusions section of this paper.

The first major contribution of this paper, described in Sec. II, is the detailed study of the behavior of $q_c(M)$ for a general underlying connectivity graph $G$. We show that $q_c(M) \sim 1/\sqrt{M}$ for $M$ large. This implies that when each node is occupied in roughly $c\sqrt{M}$ (of the $M$) layers, $c$ being a constant, spanning connectivity emerges in the $M$-layer network. We show that $c$ approaches $\sqrt{-\ln(1-p_c)}$ as $M \to \infty$, where $p_c$ is the bond-percolation threshold of $G$. In Sec. III, we find $q_c(M)$ exactly when $G$ is a large random network with an arbitrary node-degree distribution. In Sec. IV, we evaluate $q_c(M)$ numerically for various regular lattices and find an analytical lower bound for $q_c(M)$ for when $G$ is a regular kagome lattice. We show, for a general graph $G$, that $q_c(M) \lesssim \sqrt{-\ln(1-p_c)}/\sqrt{M}$, where $p_c$ is the bond-percolation threshold of $G$, and that the inequality is asymptotically tight when $M \to \infty$. Clearly, for $M = 1$, $q_c(1) \equiv q_c$, where $q_c$ is the site-percolation threshold of $G$. Therefore as $M$ goes from 1 to $\infty$, $q_c(M)$ goes from being a function solely of $q_c$ to being solely a function of $p_c$. This suggests that our multilayer percolation model forms a smooth transition between the standard site- and bond-percolation models. This leads to our second main contribution, described in Sec. V: An intriguingly close connection between the aforesaid multilayer percolation model and the well-studied problem of site-bond (or mixed) percolation—a percolation process defined on the single-layer graph $G$, in which each site and each bond in $G$ is independently activated with probability $q$ and $p$, respectively. Both models provide a smooth transition between the traditional independent and identically distributed site- and bond-percolation models. Using this connection, we show a way to translate analytical approximations to the

site-bond critical region [the region in the $(p,q)$ space where a GCC exists with high probability] that are functions solely of $p_c$ and $q_c$ to an excellent general approximation of the multilayer percolation thresholds, $q_c(M)$. We conclude the paper in Sec. VI.

## II. MULTILAYER PERCOLATION IN A LARGE GRAPH

The multilayer (random) graph $G^{(M)}$ is completely specified by the underlying connectivity graph $G$, the number of layers $M$, and the site-occupation probability $q$ (for each site in each layer). It is simple to see that the induced marginal probability, $p$, of any given bond in $G^{(M)}$ to be active is given by $p = 1-(1-q^2)^M$. Now, suppose we choose $q = c/\sqrt{M}$, with $c$ a constant. In other words, each node is occupied, on average, in $c\sqrt{M}$ layers. Then, in the limit $M \to \infty$, we have $p = 1 - \lim_{M\to\infty}(1-q^2)^M = 1 - e^{-c^2}$. If the bond activation events were statistically independent, then for $p \geqslant p_c$, where $p_c$ is the bond-percolation threshold of $G$, a giant connected component (GCC) would appear in $G^{(M)}$. Note here that $p \geqslant p_c$, in the $M \to \infty$ limit, is equivalent to $c \geqslant \sqrt{-\ln(1-p_c)}$. However, the bond activation events in $G^{(M)}$ are not independent. They have a positive spatial correlation. In other words, one bond being active makes it more likely for its neighboring bond to be active. Since $p$ is the fractional size of the edge set in the underlying graph that is active, introducing positive bond-to-bond nearest-neighbor spatial correlations, for a given $p$, implies that the active bonds will be closer together, and hence $p > p_c$ should be more than sufficient for a GCC to exist in $G^{(M)}$, thereby making $\sqrt{-\ln(1-p_c)}/\sqrt{M}$ an upper bound to the multilayer percolation threshold $q_c(M)$ for any finite $M$. Note, however, that the above argument (of why percolation should happen at a strictly lower value of $p$ for a correlated bond process) is not rigorous. We conjecture, however, that it holds true for the particular correlated bond process induced by our multilayer percolation model on an arbitrary graph $G$ that has a well-defined nontrivial independent and identically distributed bond-percolation threshold.

Clearly, for $M = 1$, $G^{(M)}$ is a simple site-percolation instance over $G$ with site-occupation probability $q$. Hence $q_c(1) = q_c$ is the site-percolation threshold of $G$. In Fig. 3, we plot the numerically evaluated values of $q_c(M)$ as a function of $M$ for a square grid. Note that as $M$ grows large, the aforesaid upper bound gets progressively tighter. This indicates that the reason which caused $\sqrt{-\ln(1-p_c)}/\sqrt{M}$ to be an upper bound (and not equal) to $q_c(M)$ in the first place—that the bond-activation events of $G^{(M)}$ are positively correlated—dwindles away in the large-$M$ limit. One can show that this is indeed true. In other words, if the single-layer site-occupation probability $q$ is chosen to be $c/\sqrt{M}$ with $c$ a constant, the induced bond-activation events in the $M$-layer graph $G^{(M)}$ progressively approach being statistically independent as $M$ increases. Therefore, in this limit, $G^{(M)}$ resembles an independent and identically distributed bond-percolation instance of $G$. Thus when $p > p_c$, the bond-percolation threshold of $G$, a GCC appears in $G^{(M)}$. Therefore, $q \sim \sqrt{-\ln(1-p_c)}/\sqrt{M}$ in the $M \to \infty$ limit, showing that the upper bound is asymptotically tight. In Theorem 1 of Appendix A, we provide a rigorous proof of the independence

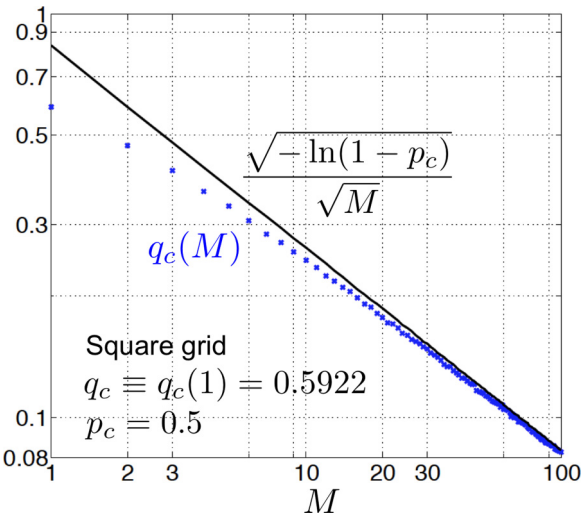


FIG. 3. Multilayer percolation thresholds for a square grid (blue crosses) were computed using the Newman-Ziff Monte-Carlo method (see Appendix G) for $M = 1, \ldots, 100$, where $q_c(1) = q_c = 0.59274605079210(2)$ is the site percolation threshold [16]. The upper bound $\sqrt{-\ln(1-p_c)}/\sqrt{M}$, plotted in black (solid), is a function only of the bond-percolation threshold $p_c = 0.5$ and is an asymptotically tight bound in the large-$M$ limit.

of the bond-activation events of $G^{(M)}$ in the $M \to \infty$, albeit only for the case when $G$ is a tree. We conjecture (and have ample numerical evidence in its favor), that this fact about the asymptotic independence of bond activation events (of $G^{(M)}$ for $q = c/\sqrt{M}$ in the $M \to \infty$ limit) holds true for any arbitrary graph $G$ that has a well-defined and nontrivial bond-percolation threshold $p_c$.

Further, recalling that the marginal probability of each bond's activation satisfies $p = 1-(1-q^2)^M$, it is simple to see that in the $M \to \infty$ limit, if the site-occupation probability $q$ is chosen to be any function of $M$ that diminishes any faster than $1/\sqrt{M}$, then all the bonds of $G^{(M)}$ are inactive with high probability, whereas if $q$ is chosen as any function of $M$ that diminishes even a little slower compared to $1/\sqrt{M}$, then all the bonds of $G^{(M)}$ are active with high probability, thereby showing that the $1/\sqrt{M}$ scaling of $q$ is a sharp connectivity threshold.

For $M = 1$, the multilayer model is equivalent to standard independent and identically distributed site percolation, and as $M$ increases, even though our multilayer construction is inherently a site-based model (i.e., defined and driven solely by site occupations), the site-occupation thresholds for long-range connectivity are determinable only from the bond-percolation threshold of the underlying connectivity graph when the number of layers grows large. The thresholds $q_c(M)$ decrease as $M$ increases, but they decrease as $c/\sqrt{M}$, where the constant $c$ is only a function of $p_c$, the bond-percolation threshold, when $M$ is large. Therefore, bond percolation naturally emerges from a multilayer site-percolation problem. This in turn suggests that there may be a deeper connection of this problem to the traditional site-bond (or mixed) percolation problem, which is a model that interpolates between the standard site- and bond-percolation models in a natural way, with each site

occupied independently with probability $q$ and each bond activated independently with probability $p$. In Sec. V, we will make this connection quantitatively rigorous, and will show how one can translate known results on the critical region for the site-bond percolation problem to the multilayer problem and vice versa.

Finally, let us see how one can further tighten the upper bound to $q_c(M)$ discussed above. The probability that any given bond in $G^{(M)}$ is active, $p = 1-(1-q^2)^M$. The bonds in $G^{(M)}$ can be thought of as generated by a positively correlated bond-percolation process on $G$ with a marginal bond probability $p$. Hence, $p > p_c$ is sufficient for a GCC to appear in $G^{(M)}$, where $p_c$ is the bond-percolation threshold of $G$. It thus follows that $q \geqslant \sqrt{1-(1-p_c)^{1/M}}$ is sufficient for percolation. Therefore, the multilayer threshold must satisfy $q_c(M) \leqslant \sqrt{1-(1-p_c)^{1/M}}$. One can further upper bound the right-hand side of the above as $\sqrt{1-(1-p_c)^{1/M}} \leqslant \sqrt{-\ln(1-p_c)}/\sqrt{M}, \forall M \geqslant 1$, to obtain $q_c(M) \leqslant \sqrt{-\ln(1-p_c)}/\sqrt{M}$. In Appendix B, we provide an additional intuition behind the above upper bound.

## III. ANALYTICAL RESULTS FOR A MULTILAYER RANDOM GRAPH

In this section, we will consider multilayer percolation on large random graphs with an arbitrary, but known, node-degree distribution. This model of random graph analysis—based on a probability-generating function (PGF) approach—is known as the *configuration model* (CM) [17,18]. The CM has found use in modeling several real-life networks that have non-Poisson distributions, such as the truncated power-law and exponential distributions [19,20]. Newman studied a multilayer random graph model, which is related but differs from ours [21].

Let $p_k$ denote the probability that a randomly selected node has degree $k$. Let $\mathcal{M}$ denote the set of $M$ layers and let $q_k$ denote the probability that a node of degree $k$ is occupied in layer $m \in \mathcal{M}$. As before, the events that a node is occupied in different layers are assumed to be independent. $p_k(1-(1-q_k)^M)$ is the probability of a node having degree $k$ and being occupied in at least one layer, and

$$F_0(x) = \sum_{k=0}^{\infty} p_k(1-(1-q_k)^M)x^k$$

is the PGF of this distribution. Let us follow a randomly chosen edge $e(u,v)$ starting from a node $u$, occupied in $n \leqslant M$ layers, to node $v$. Node $v$ has degree distribution proportional to $kp_k$ [17]. Thus the PGF of the distribution of $v$ having degree $k$ *and* being occupied in at least one of $n$ layers that $u$ is occupied in, is given by

$$F_n(x) = \frac{\sum_{k=1}^{\infty} kp_k(1-(1-q_k)^n)x^{k-1}}{z}$$

for $1 \leqslant n \leqslant M$, where $z = \sum_k kp_k$ is the average node degree.

Let $H_0(x)$ denote the PGF of the cluster size to which a randomly selected node belongs. It is easy to argue that

$$H_0(x) = 1 - F_0(1) + x\sum_{k=0}^{\infty} p_k \sum_{l=1}^{M} \binom{M}{l} q_k^l (1-q_k)^{M-l} H_l(x)^k. \tag{1}$$

Let us define $H_n(x)$ as the PGF for the size of a cluster to which a neighbor of the node belongs provided that it is occupied in at least one of the $n$ layers in which the randomly selected node is occupied. It is given by

$$H_n(x) = 1 - F_n(1) + x\sum_{k=1}^{\infty} \frac{kp_k}{z} \sum_{l=1}^{M} \left[\binom{M}{l} - \binom{M-n}{l}\right] \times q_k^l (1-q_k)^{M-l} H_l(x)^{k-1},$$

where $\binom{j}{i}$ is defined to be zero whenever $i > j$. The combinatorial term in the inner sum corresponds to the number of combinations of $l$ layers at a neighbor that overlap the $n$ layers of the original node. When $l > M-n$, all possible combinations of $l$ layers at the neighbor overlaps the $n$ layers in the original node, yielding $\binom{M}{l}$, whereas when $l \leqslant M-n$, we have to subtract out the number of $l$ layer combinations that do not overlap the $n$ layer combinations at the original node, $\binom{M-n}{l}$. We are interested in the average cluster size to which a randomly selected node belongs, which is given by $\mu_0 = H_0'(1)$,

$$\mu_0 = F_0(1) + x\sum_{k=0}^{\infty} kp_k \sum_{l=1}^{M} \binom{M}{l} q_k^l (1-q_k)^{M-l} \mu_l, \tag{2}$$

where $\mu_n = H_n'(1)$, i.e.,

$$\mu_n = F_n(1) + \sum_{k=1}^{\infty} \frac{(k-1)kp_k}{z} \times \sum_{l=1}^{M} \left[\binom{M}{l} - \binom{M-n}{l}\right] q_k^l (1-q_k)^{M-l} \mu_l.$$

Consider the case $q_k = q$. We introduce the matrix $\mathbf{A}(q) = [A_{ij}]$ with

$$A_{ij} = \begin{cases} -C\left(\binom{M}{j} - \binom{M-i}{j}\right) q^j (1-q)^{M-j} & i \neq j \\ 1 - C\left(\binom{M}{j} - \binom{M-j}{j}\right) q^j (1-q)^{M-j} & i = j \end{cases}, \tag{3}$$

where $C = \sum_k (k-1)kp_k/z$. Now $\mu = [\mu_1, \ldots, \mu_M]$ is a solution of

$$\mathbf{A}(q)\mu^T = \mathbf{b}^T, \tag{4}$$

where $\mathbf{b} = (F_1(1), \ldots, F_M(1))$. We define the critical occupancy probability, $q_c(M)$, such that when $q > q_c(M)$, there exists one infinite-size spanning cluster (or GCC) with high probability, and when $q < q_c(M)$, there exist only finite-size clusters. Assume that $C > 1$ (which is required for $G$ to have a GCC with high probability even with all nodes and bonds occupied). The size of a GCC is a constant fraction of the size of the graph. Hence, for an infinite random graph, appearance of a GCC in the $M$-layer graph is equivalent to $\mu_0$ diverging (to infinity). As Eq. (2) shows, $\mu_0$ is a constant plus a linear combination of $\{\mu_k\}$, $k = 1, \ldots, M$. Hence, at least one element of $\mu$ must diverge for $\mu_0$ to diverge. Since $\boldsymbol{b}$ is a constant vector, this can only happen if $\boldsymbol{A}$ is singular. Thus, $q_c(M)$ is given by the solution of

$$\det(\mathbf{A}(q)) = 0 \tag{5}$$

within the interval $[0,1]$. Numerically, it is easy to verify that $\det(\mathbf{A}(q))$ has a unique zero in $[0,1]$ for all $M \geqslant 1$ as long as

$C > 1$. We conjecture that this is always true. In Appendix C, we provide a rigorous proof of the fact that $q_c(M)$ is given by the smallest solution of $\det(\mathbf{A}(q)) = 0$ in the interval $(0,1)$.

For the case $M = 1$, this corresponds to finding the solution of $1 - qC = 0$, which yields the known result $q_c = 1/C$ [18]. For the case of $M = 2$, $q_c$ is the unique solution of the following polynomial:

$$C^2q^4 - C^2q^3 - Cq + 1 = 0 \tag{6}$$

within the interval $[0,1]$, which is

$$q_c(2) = \tfrac{1}{4}[a + 1 - \sqrt{3 + 2a - a^2}] \tag{7}$$

with $a = \sqrt{1 + 8/C}$. It is easy to show that there exists at least one real root in the interval $[0,1]$ provided that $C > 1$ as $\det(\mathbf{A}(0)) = 1$ and $\det(\mathbf{A}(1)) = 1 - C < 0$.

In the supercritical regime, there is one infinite-size cluster and many small finite-size clusters. The PGF of the size of a small cluster is given by $H_0(x)/H_0(1)$ with $H_0(x)$ given by (1). The average size of these clusters is $\mu_0/H_0(1)$ with $\mu_0$ given by (2). Finally, the fractional size of the giant connected component is given by $S = 1 - H_0(1)$. For the $M$-layer random graph, the fractional size of the giant connected component is given by

$$S(q,M) = 1 - (1-q)^M - \sum_{k=0}^{\infty} p_k \sum_{l=1}^{M} \binom{M}{l} q^l (1-q)^{M-l} u_l^k, \tag{8}$$

where $\boldsymbol{u} = [u_1, u_2, \ldots, u_M]^T \in [0,1]^M$ is given by the following self-consistency matrix equality:

$$\boldsymbol{u} = \boldsymbol{s} + \boldsymbol{B}\boldsymbol{v}, \tag{9}$$

where $s_l = (1-q)^l$, $v_l = f(u_l) \equiv \sum_{k=1}^{\infty} (kp_k/z) u_l^{k-1}$, and $B_{ij} = [\binom{M}{j} - \binom{M-i}{j}] q^j (1-q)^{M-j}$.

In order to verify our theory, we performed numerical simulations of layered site percolation on random graphs with up to $M = 20$ layers, and 5 million nodes, and compared with results obtained from the theory we developed above. We chose random graphs with node degrees distributed according to the truncated power law [22]

$$p_k = \begin{cases} 0 & \text{for } k = 0 \\ Dk^{-\tau} e^{-k/\kappa} & \text{for } k \geqslant 1 \end{cases}, \tag{10}$$

where $D = [\mathrm{Li}_\tau(e^{-1/\kappa})]^{-1}$ is a normalization constant, with the polylogarithm function, $\mathrm{Li}_s(x) \equiv \sum_{k=1}^{\infty} x^k/k^s$. We chose this distribution for our simulations since it is seen in a number of real-world social networks, including collaboration networks of movie actors [23] and scientific collaborations based on coauthorship of publications [24]. The pure power-law distributions seen in Internet data are also included as a special case $\kappa \to \infty$ [25].

For our numerical evaluations of $q_c(M)$, we used the Newton-Raphson method to extract the unique root of Eq. (5). Figure 4 shows an example calculation of $q_c(M)$ for a truncated power-law node degree distribution and various bounds to it discussed earlier. In order to solve for the largest cluster size $S(q,M)$, we solved Eq. (9) numerically using a multidimensional iterative fixed-point method to search for the unique solution of $\boldsymbol{u} \in [0,1]^M$. One interesting thing to note

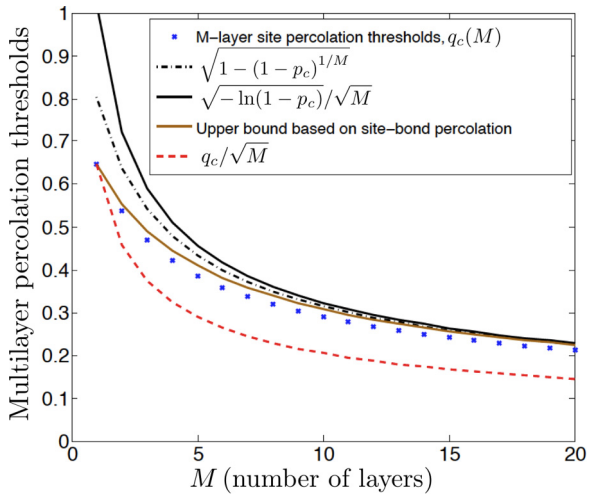


FIG. 4. Upper and lower bounds on the multilayer site-percolation thresholds for a random graph with a truncated power-law degree distribution $p_k = 0, k = 0$, $p_k = Ck^{-\tau}e^{-k/\kappa}, k \geqslant 1$, with $\kappa = 10$ and $\tau = 2.5$. The exact $q_c(M)$ values were obtained by solving Eq. (5).

is that the multilayer threshold $q_c(C,M)$ is only a function of $M$ and $C \equiv \sum_{k=1}^{\infty}(k-1)kp_k/z$, regardless of the actual distribution $\{p_k\}$. In Fig. 5, we plot $q_c(C,M)$ for different values of $C$ and $M$. The evaluations of the largest cluster size $S(q,M)$ as a function of $q$—both using the solution of Eq. (8) as well as using efficient Newman-Ziff style Monte Carlo simulations on random graph instances with 5 million nodes—for a truncated power-law node-degree distribution, with $\kappa = 10$ and $\tau = 2.5$, are summarized in Fig. 6. Excellent agreement is seen between theory and numerical simulations.

## IV. NUMERICAL RESULTS FOR REGULAR LATTICES

We numerically evaluated $q_c(M)$ for various regular lattices, including the square, triangular, kagome, and archimedian lattices. The results for a regular square grid are shown in Fig. 7 and for a regular kagome lattice in Fig. 8.

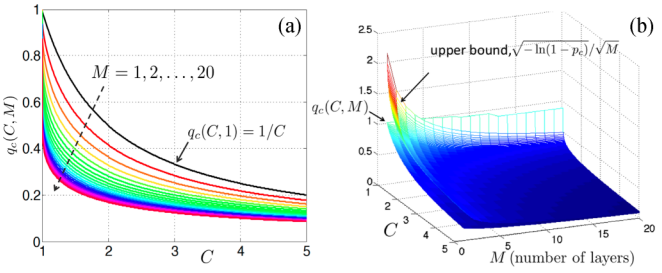


FIG. 5. (a) The multilayer threshold $q_c(C,M)$ as a function of $C$ for $M = 1,2,\ldots,20$ layers. (b) Comparing $q_c(C,M)$ with $\sqrt{-\ln(1-p_c)}/\sqrt{M}$ (with $p_c = 1/C$), which is seen to be an upper bound to $q_c(C,M)$ as argued in Appendix B. The random graphs used for these evaluations were chosen from a truncated power law node-degree distribution $p_k = 0, k = 0$, $p_k = Ck^{-\tau}e^{-k/\kappa}, k \geqslant 1$, with $\kappa = 10$ and $\tau = 2.5$.

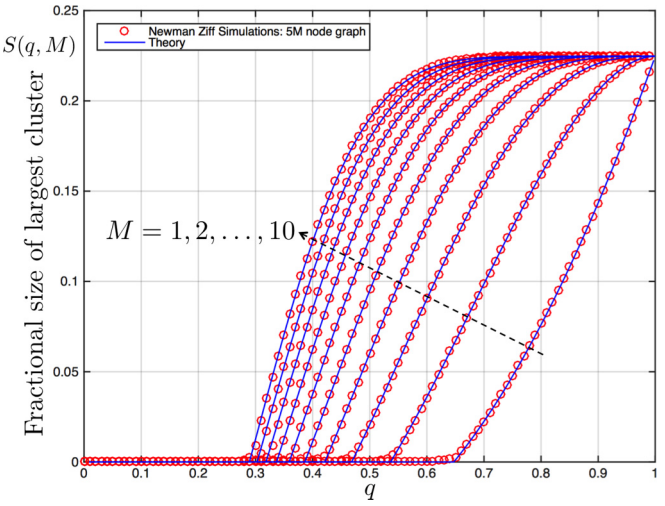


FIG. 6. Size of the spanning cluster for multilayer percolation as a function of the single-layer site-occupation probability $q$ for a random graph with a truncated power-law node-degree distribution; $p_k = 0, k = 0$, $p_k = Ck^{-\tau}e^{-k/\kappa}, k \geqslant 1$, with $\kappa = 10$ and $\tau = 2.5$. The theory plots were obtained by solving Eqs. (8) and (9). The numerical plots were obtained by Newman-Ziff style simulations, via averaging over 10 instances of a 5-million-node random graph.

The size of the largest component for the $M$-layer lattice exhibits the usual second-order phase transition at $q = q_c(M)$. In Sec. IV A, we will show a very compelling (yet, incorrect, in general) argument as to why the following general lower bound to $q_c(M)$ should hold: $q_c(M) \geqslant q_c/\sqrt{M}$, where $q_c \equiv q_c(1)$ is the site-percolation threshold. In Sec. IV B, we will prove an analytical lower bound to $q_c(M)$ for the kagome lattice—adapting the Scullard-Ziff triangle-triangle transformation technique—which is seen to be extremely close to $q_c/\sqrt{M}$.

### A. An intuitive lower bound to $q_c(M)$ that holds for most regular lattices but not in general

Consider an independent and identically distributed site-percolation process with site-occupation probability $Q$ and an $M$-layer process with single-layer site-occupation probability $q$, such that the marginal probability of a single bond to be activated in either case are identical, i.e., $Q^2 = 1 - (1 - q^2)^M$. Recall now our argument above that as $M$ increases from 1 to $\infty$, the multilayer graph $G^{(M)}$, at percolation, transitions from being identical to a pure site-percolation instance of $G$ (where bond activation events have positive spatial correlation) to a pure bond-percolation instance of $G$ (where the bond activation events are independent). Hence, one might argue that for the same total number of bonds in the respective percolating instances of a graph, if the multilayer graph percolates, that the independent and identically distributed site-occupied graph must also percolate (since the bond activations have higher positive spatial correlations in the latter). Thus, $\sqrt{1 - (1 - q_c^2)^{1/M}} \leqslant q_c(M)$. One can lower bound the left-hand side by $q_c/\sqrt{M}$, thus obtaining $q_c(M) \geqslant q_c/\sqrt{M}$.

The lower bound $q_c(M) \geqslant q_c/\sqrt{M}$ holds for various regular lattices with well-defined site-percolation thresholds [26].

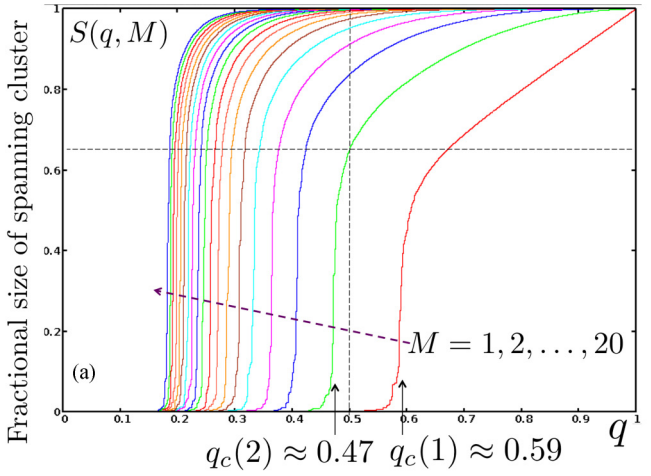


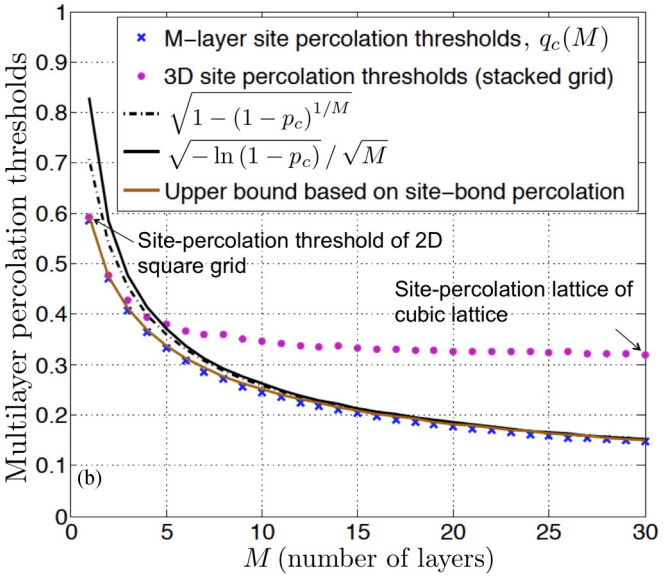


FIG. 7. Thresholds and bounds for the multilayer square lattice. Simulations performed on a 262 144-node lattice.

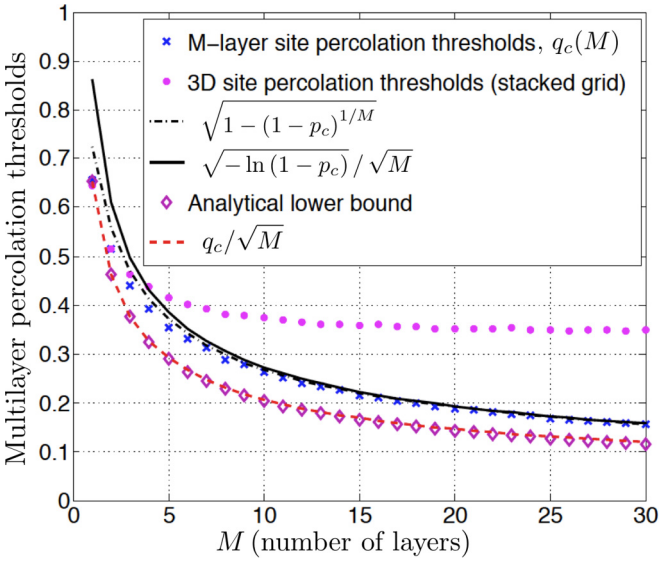


FIG. 8. Thresholds and bounds for the multilayer kagome lattice. Simulations performed on a 196 608-node lattice.

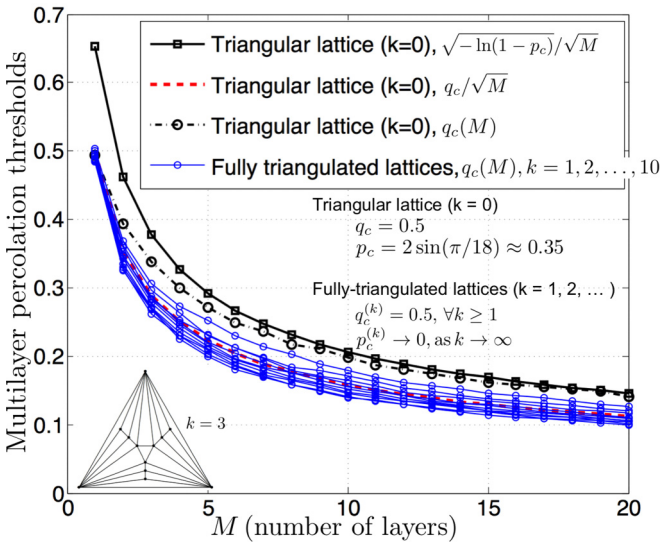


FIG. 9. Plots of $q_c(M)$ for order-$k$ fully triangulated lattices for $k = 0, 1, \ldots, 10$, where $k = 0$ corresponds to the simple triangular lattice. All these lattices have the same site-percolation threshold, $q_c^{(k)} = 0.5$, but their bond-percolation thresholds, $p_c^{(k)} \to 0$, as $k \to \infty$. The red-dashed line plots $0.5/\sqrt{M}$, therefore showing $q_c(M) \geqslant q_c/\sqrt{M}$, does not hold for these lattices with $k$ high enough.

However, the bound does break down for *fully triangulated lattices* [27], and similar graph constructions where there are many more bonds connecting a smaller number of "key" sites, for which $p_c$ can be driven to zero, with $q_c$ held constant (see Fig. 9). We conjecture that $q_c(M) \geqslant q_c/\sqrt{M}$ holds for all vertex-transitive graphs, which is backed by extensive numerical simulations.

### B. Lower bound on $q_c(M)$ for the Kagome lattice using the Scullard-Ziff triangle-triangle transformation

Numerical evaluations of $q_c(M)$ for the kagome lattice are plotted in Fig. 8. For the kagome lattice, we will now prove a lower bound for $q_c(M)$ leveraging a star-triangle transformation technique developed by Scullard and Ziff [28], which was used to find exact site-percolation thresholds for a large class of regular lattices. We will derive the following lower bound on $q_c(M)$:

$$q_c(M) \geqslant q_{\text{LB, Kagome}}(M) \tag{11}$$

for all $M \geqslant 1$, where $q_{\text{LB, Kagome}}(M)$ is the unique root of the following polynomial $f_M(q)$, in $[0,1]$:

$$f_M(q) = [(1-q)(1+q-q^2)]^M + 2(1-2q^2+q^3)^M - [(1-q)^2(1+2q)]^M - (1-q^2)^M - Mq^2. \tag{12}$$

$q_{\text{LB, kagome}}$ is seen to be extremely close, but not exactly equal, to $q_c/\sqrt{M}$, where $q_c = 1 - 2\sin\pi/18 \approx 0.6527$ is the site-percolation threshold of the kagome lattice [28] (see Fig. 8). The fact that $q_{\text{LB, kagome}} \approx q_c/\sqrt{M} \leqslant q_c(M)$ for the kagome lattice is clearly not a coincidence, given the discussion in Sec. IV A.

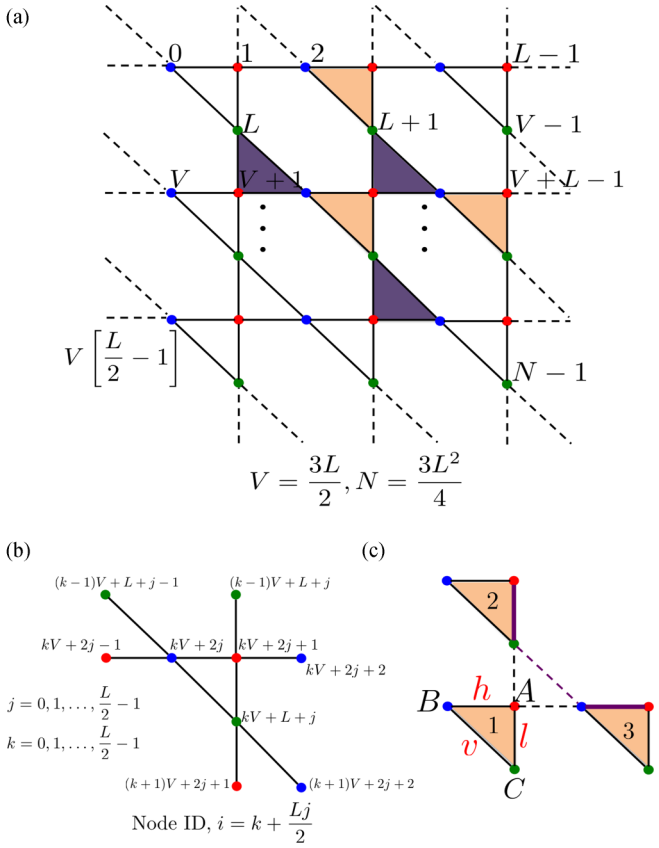


FIG. 10. (a) Casting the kagome lattice in the square grid, with one of every four nodes in the grid removed. The dashed edges are ones that "wrap around." (b) A "unit cell" of the kagome lattice showing the three node *types*, and the node numbering convention we use to construct the nearest-neighbor matrix for use in the layered grid connectivity simulations. (c) Scullard's setup for calculating the critical region for correlated-bond percolation on a triangular lattice, with bond correlations limited within each face.

The derivation of this bound uses a technique introduced by Scullard [28], who developed a site-to-bond transformation technique that leverages the duality of the triangular and honeycomb lattices to compute the critical surface for any correlated bond-percolation process on the triangular lattice where the correlations are limited to within each triangular face [28]. Figure 10(c) shows the setup. Imagine a triangular lattice formed by the shaded triangular faces, and for a moment ignore the dashed lines connecting the faces (i.e., collapse the three dashed lines into one node). The purpose of the dashed lines is to depict that there are no (bond or site existence) correlations in between faces. However, within each face, could there be a very complex correlated bond or site percolating network (but that network must be identical from face to face). Scullard showed that the critical condition for such a correlated-triangular lattice to percolate is given by the condition $P[A,B,C] = P[\bar{A},\bar{B},\bar{C}]$, where $P[A,B,C]$ is the probability that all three end nodes of a face are connected, and $P[\bar{A},\bar{B},\bar{C}]$ is the probability that none of the three nodes are connected to one another. A special case of this is that of correlated bond percolation, where each face has just three bonds $AB \equiv h$, $BC \equiv v$, and $CA \equiv l$, whose occupation

probability is given by the joint distribution $P(h,v,l)$. The percolation condition for this case translates to:

$$P(v) + P(\bar{v},h,l) = P(\bar{h},\bar{l}). \tag{13}$$

Scullard then observed that one way to generate such a correlated bond percolation on the triangular lattice—but one where the correlations do not traverse the lattice faces—is to consider a pure site percolating kagome lattice as shown in Fig. 10(a), where all the orange (light) shaded triangles are the faces of a triangular lattice where the faces are detached from one another via the dashed lines as shown in Fig. 10(c). If the site-occupation probability is $q$, it is easy to see that $P(v) = q^2$, $P(\bar{h},\bar{l}) = (1-q) + q(1-q)^2$, and $P(\bar{v},h,l) = 0$, substituting which in (13) yields a solution $q_c = 1 - 2\sin\pi/18 \approx 0.6527$. The last observation to be made is that if these orange (light) shaded triangular faces percolate (meaning there is a spanning cluster involving adjoining light-shaded faces), all the dashed bonds in Fig. 10(c) in that spanning cluster must also be occupied. Reason being, due to three-point correlations, a dashed bond will be occupied with probability 1 if two bonds on either side of it are open. More specifically, consider the bonds on triangles 2 and 3 in Fig. 10(c). Under the transformation described above, if any one bond in each triangle is occupied, then both bounding sites on each of these bonds will be occupied. But if this is true, then it follows that the dashed bond between triangles 2 and 3 will also be occupied. Thus the two occupied bonds in the faces considered above are connected to one another via the dashed bond, just by virtue of being occupied themselves. Thus, by inserting the separating dashed triangles between the triangular faces, we have preserved the conditions for Eq. (13) to be valid—that of neighboring triangular faces to be independent. Hence, $q_c = 1 - 2\sin\pi/18$, via this construction, is the pure site-percolation threshold of the kagome lattice [28].

Now consider applying the above technique to the $M$-layer merged kagome lattice. We can still use Eq. (13), but it will only give a necessary condition for the $M$-layer lattice to percolate, since the existence of one bond each in triangles 2 and 3 will no longer necessitate the dashed bond separating them to be occupied, because the end nodes of the dashed line could now be occupied in nonintersecting layer sets. Therefore, the solution to (13) will yield a lower bound to $q_c(M)$—the minimum value of single-layer site occupation probability such that the $M$-layer lattice will percolate. With a little combinatorics (detailed arguments omitted), one can calculate the following probabilities:

$$P(v) = Mq^2, \tag{14}$$

$$P(\bar{h},\bar{l}) = (1-q)^M(1+q-q^2)^M, \quad \text{and} \tag{15}$$

$$P(\bar{v},h,l) = (1-q^2)^M + [(1-q)^2(1+2q)]^M - 2(1-2q^2+q^3)^M, \tag{16}$$

which, after substituting into Eq. (13), one obtains the condition stated above to calculate the lower bound, $q_{\text{LB, Kagome}}(M) \leqslant q_c(M)$. For completeness, we prove in Appendix D that $f_M(q)$ has a unique root in $(0,1)$.

The lower bound $q_{\text{LB, kagome}}(M)$ is seen to be tantalizingly close to $q_c(1)/\sqrt{M}$ (plotted with red dashes in Fig. 8), but the two are not exactly equal. The magenta dots in Fig. 8 plot the site-percolation threshold $q_{c,\text{stacked}}(M)$ of the three-dimensional (3D) stacked kagome lattice (which is of interest due to its interesting magnetic properties [29,30]). The simulations indicate that the site-percolation threshold for a 50-layer stacked lattice is roughly $q_{c,\text{stacked}}(50) \approx 0.366$. This is in agreement with the numerically evaluated site-percolation threshold of the infinite stacked kagome lattice, $q_{c,\text{stacked}}(\infty) = 0.3346(4)$ [31].

One interesting thing to note is that when $q > q_{\text{LB, Kagome}}(M)$, by the Scullard argument, all the orange (light) shaded triangles in the infinite multilayer Kagome lattice [see Fig. 10(a)] will form a spanning cluster amidst themselves, i.e., assuming the purple (dark) shaded triangles do not come in the way of a pair of occupied nearest-neighbor light-shaded triangles to get "connected." But then, because of symmetry, when $q > q_{\text{LB, Kagome}}(M)$, all the purple (dark) shaded triangles should also have a spanning cluster ("ignoring" the light-shaded triangles). So, when $q$ is in the regime, $q_{\text{LB, Kagome}}(M) < q < q_c(M)$, the light-shaded triangles percolate, *and* the dark-shaded triangles percolate, but the full multilayer Kagome lattice does not percolate, which happens only when $q \geqslant q_c(M)$. This situation has some semblance with the notion of *explosive percolation* that has been studied recently [32].

## V. RELATIONSHIP WITH SITE-BOND PERCOLATION AND ANALYTICAL APPROXIMATIONS TO THE MULTILAYER THRESHOLDS

As discussed above, the $M$-layer graph $G^{(M)}$ transitions from resembling site percolation to resembling bond percolation as $M$ goes from 1 to $\infty$. Joint *site-bond* percolation is a well-studied extension of site and bond percolation [33–35], which is a more natural bridge between site and bond percolation, where each site is occupied and each bond is activated independently with probabilities $Q$ and $P$, respectively, and a path or a cluster can only be formed using occupied sites *and* activated bonds. This suggests that the two percolation models should be connected. The boundary separating the subcritical and supercritical phases for site-bond percolation, the critical line $f_c(P,Q) = 0$, is not known exactly for any lattice. In Sec. V A, we will establish a quantitative connection between site-bond and multilayer percolation and show how one can translate the site-bond critical line $f_c(P,Q) = 0$ to an upper bound to $q_c(M)$, which is tight both at $M = 1$ and at $M \to \infty$. In Sec. V B, we will leverage a good approximation to the site-bond critical line to develop excellent approximations to $q_c(M)$ for general regular lattices that are only a function of the site- and bond-percolation thresholds $q_c$ and $p_c$ of the respective lattices.

### A. Translating the site-bond critical boundary to a tight upper bound to the multilayer threshold

The multilayer graph can be thought of as being generated by a site-bond percolation process, where sites are independently occupied with probability $Q(q,M) = 1-(1-q)^M$ and conditioned on two nearest-neighbor sites being both occupied, the bond between them being active with probability

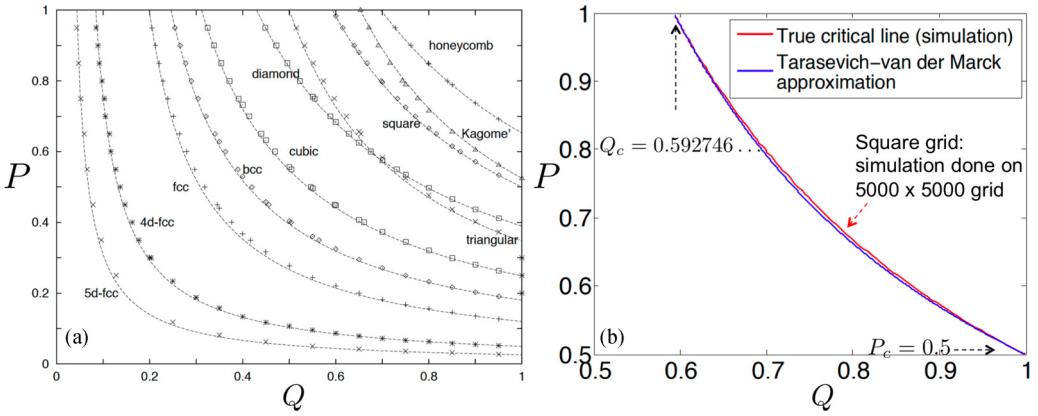


FIG. 11. Site-bond critical regions: Comparison between true critical region and the Tarasevich-van der Marck approximation. (a) Figure from Ref. [35]; (b) refined simulations for the critical region for the square lattice using Newman-Ziff method on a 25-million-node grid.

$P(q,M) = [1-(1-q^2)^M]/[1-(1-q)^M]^2$. In other words, $P$ is the probability that two sites are occupied in at least one common layer, given they are both occupied. For $M = 1$, we get $P = 1$ as expected and this reduces to pure site percolation. For $M > 1$, there is one subtle difference between site-bond percolation and multilayer percolation mapped on the site-bond model as described above: the nearest-neighbor bond activations have greater spatial correlation in multilayer percolation as compared to site-bond percolation, conditioned on an instance of the underlying independent and identically distributed site process generated with site-occupation probability $Q(q,M)$. For example, given that three successive sites on a path are occupied, in the $(P,Q)$ site-bond process, the probability that both bonds between those three sites are occupied is $P^2$, whereas in multilayer percolation, the probability that both of those bonds are occupied (again conditioned on all three sites being occupied) is greater than $P^2$. This suggests that if the site-bond process on a graph $G$ percolates for a given $(P,Q)$, then for the same $(P,Q)$ value (translated to $q$ and $M$ as above), the multilayer percolation process on $G$ should also percolate. This suggests that if we know the site-bond critical line $f_c(P,Q) = 0$ for a graph, and solve for $q^*(M)$ by substituting $P(q,M)$ and $Q(q,M)$ into the critical line equation, then the solution $q^*(M)$ will be an upper bound to the true multilayer percolation threshold $q_c(M)$ for that graph. If the critical line is only available numerically, then we can find $q^*(M)$ by solving for the intersection of $f_c(P,Q) = 0$ with $PQ^2 = 1-(1-q^2)^M$. Note that the above argument is not a formal proof that $q^*(M) \geqslant q_c(M)$, but we have not found a single graph for which this upper bound is violated. The brown solid lines in Fig. 7(b) and Fig. 5 plot this upper bound for the square grid and a random graph, respectively. This upper bound, unlike the upper bound $q_c(M) \leqslant \sqrt{-\ln(1-p_c)}/\sqrt{M}$, is tight both at $M = 1$ and at $M \to \infty$, since it interpolates between pure-site and pure-bond percolation, which is a characteristic of both multilayer and site-bond percolation.

For a random graph with degree distribution $\{p_k\}$, the critical line is a hyperbola given by $f_c(P,Q) = PQ - 1/C = 0$, with $C = \sum_k (k-1)kp_k/z$, $z = \sum_k kp_k$. The following thus readily follows: For multilayer site percolation on a random graph with degree distribution $\{p_k\}$, the $M$-layer thresholds satisfy, $q_c(M) \leqslant q_{\mathrm{UB,Random-Graph}}$, where $q_{\mathrm{UB,Random-Graph}}$ is given by the unique root of the following polynomial $g_M(q)$, in $(0,1]$:

$$g_M(q) = (1-q^2)^M - \frac{1}{C}(1-q)^M + (1/C) - 1. \qquad (17)$$

See Appendix E for proof of uniqueness of the root.

### B. A general approximation to $q_c(M)$ that is only a function of $p_c$ and $q_c$ of a regular lattice

Yanuka and Englman proposed an approximation to $f_c(P,Q) = 0$ for regular lattices purely in terms of $q_c$ and $p_c$ [34], which was later improved by Tarasevich and van der Marck [35], who showed that the critical line $f_c(P,Q) = 0$ for any lattice is well approximated by $P(Q+A) = B$, with $A = (p_c - q_c)/(1-p_c)$ and $B = p_c(1-q_c)/(1-p_c)$ (see Fig. 11). Therefore, as per the discussion above, it is evident that substituting $Q = 1-(1-q)^M$ and $P = [1-(1-q^2)^M]/[1-(1-q)^M]^2$ into $P(Q+A) = B$ would result in a good approximation to $q_c(M)$ for a general lattice whose site- and bond-percolation thresholds ($q_c$ and $p_c$, respectively) are known. We thus have the following.

The multilayer threshold $q_c(M)$ for any graph $G$ is well approximated by the unique solution of the following polynomial equation $f_{\mathrm{SB}}(q) = 0$ in $(0,1]$, where

$$f_{\mathrm{SB}}(q) = [1-(1-q^2)^M][1-(1-q)^M + A] - B[1-(1-q)^M]^2,$$

where $A(p_c,q_c)$ and $B(p_c,q_c)$ are as stated above.

The proof that $f_{\mathrm{SB}}(q)$ has a unique root in $(0,1)$ for any given $p_c$, $q_c$, and $M$ is given in Appendix F. Figure 12 shows the agreement of the approximations to $q_c(M)$ with the true thresholds $q_c(M)$ for the square, triangular, and kagome lattices. Note that the approximations are neither strictly an upper nor a lower bound to $q_c(M)$ in general. The fact that the analytical approximations to $f_c(P,Q) = 0$ are lower estimates of the true critical line counters the fact that the translation of the true site-bond critical line should give us an upper bound to $q_c(M)$—thereby producing very good estimates of $q_c(M)$.

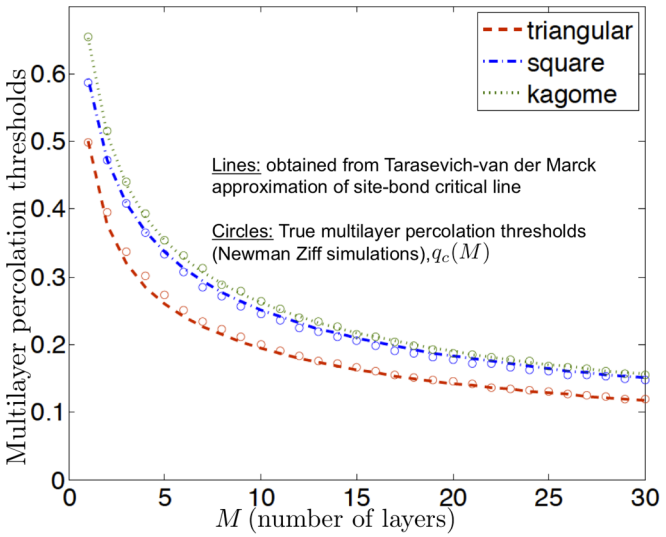


FIG. 12. Comparison of $q_c(M)$—for the square, triangular, and kagome lattices—to approximations obtained by using the Tarasevich-van der Marck approximations to the site-bond threshold.

## VI. CONCLUSIONS

In this paper, we studied the emergence of long-range connectivity in a specific kind of multilayer network, which have the following two properties: (1) each node in the multilayer network is a physical entity that is common to each of the $M$ layers, where the layers correspond to co-existing means of connectivity and each node may only be active in a subset of all the layers, and (2) each network layer is a subgraph of a common underlying connectivity graph $G(V,E)$, obtained by making each node in $G$ active in any given layer independently with probability $q$. The edge set $E$ defines all the possible connections the nodes in $V$ may have, some of which may remain dormant in a particular instance of the multilayer network, if the nodes an edge connects are not active in a common layer.

We studied the properties of $q_c(M)$, the threshold value of the single-layer site-occupation probability $q$, when a spanning cluster begins to emerge in the $M$-layer network. We showed that $q_c(M) = \Theta(1/\sqrt{M})$, i.e., for the $M$-layer network to have long-range connectivity, each node must be active in $c\sqrt{M}$ layers on an average. We also showed that $c \to \sqrt{-\ln(1-p_c)}$ as $M \to \infty$, where $p_c$ is the bond-percolation threshold of $G$. This arises from a realization that if each node is active in $\propto \sqrt{M}$ layers, then the induced bond activation events approach being independent and identically distributed as $M$ becomes large. We derived $q_c(M)$ exactly for random graphs with arbitrary degree distributions. Since $q_c(1) \equiv q_c$ is the site-percolation threshold of $G$, the observation that $q_c(M)$ only depends on the bond-percolation threshold $p_c$ when $M$ is large led us to find a close relationship between the above multilayer percolation model and site-bond percolation, which we used to translate a known approximation to the boundary of the site-bond critical region to an excellent approximation of $q_c(M)$.

One may consider various extensions of our work. For ease of analysis, we assumed the underlying population for generating each network layer to be identical, which could be relaxed in order to study a wider class of multilayer networks. Even if the assumption about the underlying connectivity graph is accurate, the occupation probability of each node need not be the same in each layer. One could consider alternative multilayer connectivity models driven by the application, such as the compatibility across communication modes or technologies, information traversal hierarchy (e.g., in military networks), causality of information flow (in temporally evolving networks) where the vertical axis in Fig. 1 would represent time, or stacked lattices (where nodes connect across nearest-neighbor layers only). Furthermore, the activity of users in each layer may evolve over time, and messages could be stored at a node and forwarded to a neighboring node at a later time instant when both nodes are simultaneously active in a common layer. It would also be interesting to analyze multilayer versions of the *susceptible-infected-recovered* (SIR) model of epidemic spread, such as in analyzing vaccination strategies with limited supplies when nodes can carry multiple viral strains. Finally, it may be interesting to incorporate "edge weights" (i.e., the information about how many layers an edge is active in) into the structural analysis. This will help study the "robustness" of the giant component or that of a multilayer path. Our analysis in this paper was limited to the first-order effect—connectivity—which does not pay heed to the "strength" of an edge. Aside from robustness analysis, another interesting reason to consider edge weights would be to study multiple simultaneous interlayer information flows. In such a scenario, if an edge that bridges two highly connected islands is only active in one layer, it may become a "bottleneck" link, whereas being active in several layers would make the multiflow information traversal easier.

## ACKNOWLEDGMENTS

S.G. thanks Hari Krovi for useful discussions and Robert Ziff for providing useful comments on an early draft and for pointing out prior results on site-percolation thresholds for the stacked Kagome lattice. P.N. thanks Alain Jean-Marie for helping prove the uniqueness of the root for $f_{\mathrm{SB}}(q) = 0$. The authors thank an anonymous referee for noting a small discrepancy in Fig. 6, which helped identify a numerical issue in our Newman-Ziff simulations. This research was sponsored by the U.S. Army Research Laboratory (ARL) and the U.K. Ministry of Defense (MoD) and was accomplished under Agreements No. W911NF-06-3-0002.1 (U.S. ARL and UK MoD NIS-ITA) and No. W911NF-09-2-0053 (US ARL NS-CTA). C.C. acknowledges useful discussions with Dennis Goeckel and support from the UMASS Amherst NSF Grant No. CNS-1018464. This document does not contain technology or technical data controlled under either the U.S. International Traffic in Arms Regulations or the U.S. Export Administration Regulations.

## APPENDIX A: THE CONSTANT $c$ IN THE ASYMPTOTIC SCALING LAW FOR THE MULTILAYER SITE-PERCOLATION THRESHOLD, $q_c(M) \sim c/\sqrt{M}$

In Sec. II, we showed that for our multilayer network defined on any underlying graph $G$, the threshold on the

single-layer site-occupation probability which, when exceeded, makes a GCC appear in the $M$-layer network $G^{(M)}$, satisfies $q_c(M) \sim c/\sqrt{M}$ for $M$ large. We also argued that if $q$ is chosen to be any function that diminishes faster than $1/\sqrt{M}$, then all the bonds of $G^{(M)}$ are inactive with with high probability, whereas if $q$ is chosen as any function of $M$ that diminishes even a little slower compared to $1/\sqrt{M}$, then all the bonds of $G^{(M)}$ are active with high probability, thereby showing that the $1/\sqrt{M}$ scaling of $q$ is a sharp connectivity threshold for the $M$-layer network. In Sec. II, we also presented an intuitive argument to show that $c = \sqrt{-\ln(1-p_c)}$, where $p_c$ is the bond-percolation threshold of $G$. In this Appendix, we will prove this rigorously for the case when $G$ is a tree. We believe that this result is true for an arbitrary graph $G$ (i.e., even one that has cycles) as long as $G$ has a well-defined bond-percolation threshold. We leave the extension of the proof below, for this general case, for future work.

*Theorem 1* **[Multilayer site percolation: The constant in the scaling].** For a homogenous multilayer network formed via merging $M$ random site-percolation instances of a graph $G$ with a tree topology and site-occupation probability $q$, the threshold $q_c(M)$ on the single-layer site-activation probability such that a spanning cluster appears satisfies: $q_c(M) \sim c/\sqrt{M}$ as $M \to \infty$, where $c = \sqrt{-\ln(1-p_c)}$ and $p_c$ is the bond-percolation threshold of $G$.

*Proof.* Given the discussion in Sec. II, the only additional argument that we need in order to complete the proof is the fact that when $q = aM^{-1/2}$ for a constant $a > 0$, the bond activation events in the $M$-layer graph $G^{(M)}$ are statistically independent, when $M \to \infty$. In Proposition 1 below, we will prove this bond independence statement for the case when $G$ is a tree. Let us first begin with a few preliminaries.

If $(Z,N,q)$ is a binomial rv with mean $\mu = Nq$, then the following Chernoff's bounds hold:

$$P(Z \leqslant (1-\delta)\mu) \leqslant e^{-\mu\delta^2/2} \tag{A1}$$

and

$$P(Z \geqslant (1+\delta)\mu) \leqslant e^{-\mu\delta^2/3} \tag{A2}$$

for any $\delta \in (0,1)$. From the above we get

$$P((1-\delta)\mu \leqslant Z \leqslant (1+\delta)\mu) \geqslant 1 - e^{-\mu\delta^2/3} - e^{-\mu\delta^2/2}. \tag{A3}$$

For any mapping $f : \{0,1,\ldots\} \to [0,1]$, define

$$F_f(N) = \sum_{n=0}^{N} \binom{N}{n} q^n (1-q)^{N-n} f(n). \tag{A4}$$

*Lemma 1.* For any $\delta \in (0,1)$

$$g_f(N,\delta)\left(1 - 2e^{-\mu\delta^2/3}\right) \leqslant F_f(N) \leqslant h_f(N,\delta) + 2e^{-\mu\delta^2/3} \tag{A5}$$

with

$$g_f(N,\delta) := \min_{\lfloor(1-\delta)\mu\rfloor \leqslant n \leqslant \lceil(1+\delta)\mu\rceil} f(n), \tag{A6}$$

$$h_f(N,\delta) := \max_{\lfloor(1-\delta)\mu\rfloor \leqslant n \leqslant \lceil(1+\delta)\mu\rceil} f(n). \tag{A7}$$

*Proof.* Fix $\delta \in (0,1)$. We have

$$F_f(N) = S_{f,1}(N,\delta) + S_{f,2}(N,\delta) + S_{f,3}(N,\delta)$$

with

$$S_{f,1}(N,\delta) = \sum_{n=\lfloor(1-\delta)\mu\rfloor}^{\lceil(1+\delta)\mu\rceil} \binom{N}{n} q^n (1-q)^{N-n} f(n)$$

$$S_{f,2}(N,\delta) = \sum_{n=0}^{\lfloor(1-\delta)\mu\rfloor - 1} \binom{N}{n} q^n (1-q)^{N-n} f(n)$$

$$S_{f,3}(N,\delta) = \sum_{n=\lceil(1+\delta)\mu\rceil+1}^{N} \binom{N}{n} q^n (1-q)^{N-n} f(n).$$

(a) *Upper bound.*
With (A7) we get

$$S_{f,1}(N,\delta) \leqslant h_f(N,\delta) \sum_{n=0}^{N} \binom{N}{n} q^n (1-q)^{N-n} = h_f(N,\delta),$$

$$S_{f,2}(N,\delta) \leqslant \sum_{n=0}^{\lfloor(1-\delta)\mu\rfloor - 1} \binom{N}{n} q^n (1-q)^{N-n} \quad \text{since } f \in [0,1]$$

$$= P(Z \leqslant \lfloor(1-\delta)\mu\rfloor - 1)$$

$$\leqslant P(Z \leqslant (1-\delta)\mu) \leqslant e^{-\mu\delta^2/2},$$

by using Chernoff's bound (A1), and

$$S_{f,3}(N,\delta) \leqslant \sum_{n=\lceil(1+\delta)\mu\rceil+1}^{N} \binom{N}{n} q^n (1-q)^{N-n}$$

$$= P(Z \geqslant \lceil(1+\delta)\mu\rceil + 1)$$

$$\leqslant P(Z \geqslant (1+\delta)\mu) \leqslant e^{-\mu\delta^2/3},$$

by using Chernoff's bound (A2). In summary,

$$F_f(N) \leqslant h_f(N,\delta) + 2e^{-\mu\delta^2/3}. \tag{A8}$$

(b) *Lower bound.*
With (A6) we get

$$F_f(N) \geqslant S_{f,1}(N,\delta)$$

$$\geqslant g_f(N,\delta) \sum_{n=\lfloor(1-\delta)\mu\rfloor}^{\lceil(1+\delta)\mu\rceil} \binom{N}{n} q^n (1-q)^{N-n}$$

$$= g_f(N,\delta)(P(\lfloor(1-\delta)\mu\rfloor \leqslant Z \leqslant \lceil(1+\delta)\mu\rceil)$$

$$\geqslant g_f(N,\delta)\left(1 - e^{-\mu\delta^2/2} - e^{-\mu\delta^2/3}\right) \quad \text{from (A3)}$$

$$\geqslant g_f(N,\delta)\left(1 - 2e^{-\mu\delta^2/3}\right). \tag{A9}$$

Combining (A8) and (A9) yields (A5). ■

Throughout $\bar{a} = 1 - a$ for any $a \in [0,1]$. Let us represent a tree $T$ as $T = (v, T_1, \ldots, T_L)$, where $T_l$ is a subtree hanging off the root $v$. We denote by $v_l$ the root of subtree $T_l$.

Let us represent the state of a tree $X(T)$ by $X(T) = \{(X_1, X(T_1)), \ldots, (X_L, X(T_L))\}$ where $X_l \in \{0,1\}$ is the state of link $(v, v_l)$ between $v$ and subtree $T_l$. Here $X_l = 0$ means the

link is inactive; otherwise, it is active. Last, let $T = \emptyset$ denote the empty tree ($L = 0$). Suppose that there are $M$ layers and let $q$ be the probability that a site is occupied in one layer.

Let $Q_{T,x(T)} = P(X(T) = x(T))$ denote the probability that the link state of the tree is $x(T)$. It can be expressed as

$$Q_{T,x(T)} = \sum_{n=0}^{M} \binom{M}{n} q^n (1-q)^{M-n} Q_{T,x(T)}(n). \tag{A10}$$

Here $Q_{T,x(T)}(n)$ is the probability that the link state of tree $T$ is $x(T)$ conditioned on the number of occupied layers at the root being $n$. It satisfies the recursion:

$$\begin{aligned} &Q_{T,x(T)}(n) \\ &= \prod_{l=1}^{L} \Bigg\{ \bar{x}_l (1-q)^n \sum_{i=0}^{M-n} \binom{M-n}{i} q^i (1-q)^{M-n-i} \\ &\quad \times Q_{T_l,x(T_l)}(i) + x_l \sum_{j=1}^{n} \binom{n}{j} q^j (1-q)^{n-j} \sum_{i=0}^{M-n} \binom{M-n}{i} \\ &\quad \times q^i (1-q)^{M-n-i} Q_{T_l,x(T_l)}(i+j) \Bigg\}, \end{aligned} \tag{A11}$$

with $x(T) = ((x_1, x(T_1)), \ldots, (x_L, x(T_l)))$. By convention, $Q_{T_l,x(T_l)}(\cdot) = 1$ if $T_l$ is only composed of the node $v_l$.

In the right-hand side of (A11) the term $\bar{x}_l(\bar{q}^n \sum_{i=0}^{M-n} \binom{M-n}{i} q^i (1-q)^{M-n-i} Q_{T_l,x(T_l)}(i)$ accounts for the fact that if link $(v, v_l)$ is inactive ($x_l = 0$), then node $v_l$ cannot share any layer with node $v$ (this occurs with probability $(1-q)^n$) but otherwise can have any other layers among the $M-n$ remaining layers; the term $x_l \sum_{i=0}^{M-n} \binom{M-n}{i} q^i (1-q)^{M-n-i} \sum_{j=1}^{n} \binom{n}{j} q^j (1-q)^{n-j} Q_{T_l,x(T_l)}(i+j)$ accounts for the fact that if link $(v, v_l)$ is active ($x_l = 1$), then node $v_l$ must share at least one layer with node $v$ but otherwise can take any other layers. The product accounts for the fact that subtrees $T_1, \ldots, T_L$ have stochastically independent behavior conditioned on the state, $n$, of node $v$.

In particular,

$$Q_{T,x(T)}(n) = \prod_{l=1}^{N} [\bar{x}_l (1-q)^n + x_l (1 - \bar{q}^n)] \tag{A12}$$

if $T_l = (v_l)$ for $l = 1, \ldots, L$ or, equivalently, if $T$ is only composed of its root $v$ and of its leaves $v_1, \ldots, v_L$.

Interverting the last two sums in (A11) gives

$$\begin{aligned} &Q_{T,x(T)}(n) \\ &= \prod_{l=1}^{L} \Bigg\{ \bar{x}_l (1-q)^n \sum_{i=0}^{M-n} \binom{M-n}{i} q^i (1-q)^{M-n-i} \\ &\quad \times Q_{T_l,x(T_l)}(i) + x_l \sum_{i=0}^{M-n} \binom{M-n}{i} q^i (1-q)^{M-n-i} \\ &\quad \times \sum_{j=1}^{n} \binom{n}{j} q^j (1-q)^{n-j} Q_{T_l,x(T_l)}(i+j) \Bigg\}. \end{aligned} \tag{A13}$$

*Proposition 1.* Assume that $q = aM^{-1/2}(1 + o(1))$. Then,

$$\begin{aligned} \lim_{M\to\infty} Q_{T,x(T)} = \prod_{l=1}^{L} \Big\{ &\left(\bar{x}_l e^{-a^2} + x_l \left(1 - e^{-a^2}\right)\right) \\ &\times \prod_{j=1}^{n_l} \left(\bar{x}_{l,j} e^{-a^2} + x_{l,j} \left(1 - e^{-a^2}\right)\right) \Big\}, \end{aligned} \tag{A14}$$

with $x(T) = ((x_1, x(T_1)), \ldots, (x_L, x(T_L)))$, $n_l$ the number of links in the subtree $T_l$, and $(x_{l,j}, j = 1, \ldots, n_l)$ the state of these links.

Equation (A14) shows that the links become stochastically independent of each other as $M$ becomes large.

*Proof.* Throughout we assume that $q = aM^{-1/2}[1 + o(1)]$.

Consider first the tree $T = (v, v_1, \ldots, v_N)$ of height one, composed of the root $v$ and of the leaves $v_1, \ldots, v_N$. From (A12) we see that

$$\lim_{M\to\infty} Q_{T,x(T)}(f(M)) = \prod_{l=1}^{L} \left[\bar{x}_l e^{-a^2} + x_l \left(1 - e^{-a^2}\right)\right] \tag{A15}$$

for any mapping $f$ such that $f(M) = aM^{-1/2}[1 + o(1)]$.

Let $T = ((x_1, x(T_1)), \ldots, (x_L, x(T_L)))$ be an arbitrary tree, with $n_l$ the number of links in the subtree $T_l$ and $(x_{l,j}, j = 1, \ldots, n_l)$ the state of these links. We will prove that:

$$\begin{aligned} \lim_{M\to\infty} Q_{T,x(T)}(f(M)) = &\prod_{l=1}^{L} \left[\bar{x}_l e^{-a^2} + x_l \left(1 - e^{-a^2}\right)\right] \\ &\times \prod_{j=1}^{n_l} \left[\bar{x}_{l,j} e^{-a^2} + x_{l,j} \left(1 - e^{-a^2}\right)\right] \end{aligned} \tag{A16}$$

for any mapping $f$ such that $f(M) = aM^{-1/2}[1 + o(1)]$.

We use an induction argument to prove (A16). We know from (A15) that (A16) is true for any tree of height 1. Assume that it is true for any tree of height $k$ and let us prove that it is still true for a tree of height $k+1$.

Let $T = ((x_1, x(T_1)), \ldots, (x_L, x(T_L)))$ be an arbitrary tree of height $k+1$, with $n_l$ the number of links in the subtree $T_l$ and $(x_{l,j}, j = 1, \ldots, n_l)$ the state of these links. Subtrees $(T_l)_l$ have height at most $k$ with at least one having a height of $k$.

Define $\mu(m) = mq$ and $\delta(m) = 1/m^{\alpha}$ with $0 < \alpha < 1/4$. From (A10), (A13), and Lemma 1 we obtain the following two-sided bounds for $Q_{T,x(T)}$ and $Q_{T,x(T)}(n)$:

$$\begin{aligned} &Q_{T,x(T)}(a_0(M))(1 - \gamma(M)) \\ &\quad \leqslant Q_{T,x(T)} \leqslant Q_{T,x(T)}(a_1(M)) + \gamma(M) \end{aligned} \tag{A17}$$

with

$$\begin{aligned} a_0(m) &:= \arg\min\{Q_{T,x(T)}(i) : \alpha(m) \leqslant i \leqslant \beta(m)\} \\ a_1(m) &:= \arg\min\{Q_{T,x(T)}(i) : \alpha(m) \leqslant i \leqslant \beta(m)\}, \end{aligned}$$

and

$$\prod_{l=1}^{l}\left(\bar{x}_l\bar{q}^n Q_{T_l,x(T_l)}(b_{l,0}(M-n))+x_l(1-\bar{q}^n)(1-\gamma(M-m))^L\right)$$
$$\leqslant Q_{T,x(T)}(n)\leqslant\prod_{l=1}^{L}\left(\bar{x}_l\bar{q}^n Q_{T_l,x(T_l)}(b_{l,1}(M-n))\right.$$
$$\left.+x_l(1-\bar{q}^n)Q_{T_l,x(T_l)}(c_{l,1}(M-n))+2\gamma(M-n)\right) \tag{A18}$$

with

$$b_{l,0}(m):=\arg\min\left\{Q_{T_l,x(T_l)}(i):\alpha(m)\leqslant i\leqslant\beta(m)\right\}$$
$$b_{l,1}(m):=\arg\max\left\{Q_{T_l,x(T_l)}(i):\alpha(m)\leqslant i\leqslant\beta(m)\right\}$$
$$c_{l,0}(m):=\arg\min\left\{Q_{T_l,x(T_l)}(i+r):\alpha(m)\leqslant i\leqslant\beta(m),\right.$$
$$\left.1\leqslant r\leqslant m\right\}$$
$$c_{l,1}(m):=\arg\max\left\{Q_{T_l,x(T_l)}(i+r):\alpha(m)\leqslant i\leqslant\beta(m),\right.$$
$$\left.1\leqslant r\leqslant m\right\},$$

where $\alpha(m):=\lfloor(1-\delta(m))\mu(m)\rfloor$, $\beta(m):=\lceil(1+\delta(m))\mu(m)\rceil$, $\gamma(m):=2e^{-\mu(m)\delta(m)^2/3}$.

Since $b_{l,0}(M-n), c_{l,0}(M-n), b_{l,1}(M-n)$, and $c_{l,1}(M-n)$ all behave as $a\sqrt{M}(1+o(1))$ when $n=a\sqrt{M}[1+o(1)]$ and $M$ is large, we can use the induction assumption to replace $n$ by $a\sqrt{M}[1+o(1)]$ in both the lower bound and the upper bound in (A18). By letting now $M\to\infty$ in the latter expressions, we obtain from the induction hypothesis that both bounds converge to $\prod_{l=1}^{L}\{(\bar{x}_l e^{-a^2}+x_l(1-e^{-a^2}))\prod_{j=1}^{n_l}(\bar{x}_{l,j}e^{-a^2}+x_{l,j}(1-e^{-a^2}))\}$, which proves that

$$\lim_{M\to\infty}Q_{T,x(T)}(f(M))=\prod_{l=1}^{L}\left\{\left(\bar{x}_l e^{-a^2}+x_l\left(1-e^{-a^2}\right)\right)\right.$$
$$\left.\times\prod_{j=1}^{n_l}\left(\bar{x}_{l,j}e^{-a^2}+x_{l,j}\left(1-e^{-a^2}\right)\right)\right\}. \tag{A19}$$

From $a_0(M)=a\sqrt{M}[1+o(1)]$ and $a_1(M)=a\sqrt{M}[1+o(1)]$, (A19), and the bounds in (A17), we finally get

$$\lim_{M\to\infty}Q_{T,x(T)}=\prod_{l=1}^{L}\left\{\left[\bar{x}_l e^{-a^2}+x_l\left(1-e^{-a^2}\right)\right]\right.$$
$$\left.\times\prod_{j=1}^{n_l}\left[\bar{x}_{l,j}e^{-a^2}+x_{l,j}\left(1-e^{-a^2}\right)\right]\right\}, \tag{A20}$$

which concludes the proof. ■

This concludes the proof of Theorem 1, for the case when $G$ is a tree. ■

*Remark 1.* We believe the asymptotic independence property holds even when $G$ is an arbitrary graph and that $c$ takes the same value as above. This is supported by extensive simulations.

*Remark 2.* In Appendix B, we argue (without proof) that for any (finite) $M\geqslant 1$, $q_c(M)\leqslant\sqrt{-\ln(1-p_c)}/\sqrt{M}$.

Finally, it is intuitive that the cluster sizes must grow with the number of layers $M$. In other words, the single-layer site-occupation probability $q$ at which the $M$-layer network percolates (i.e., has a spanning cluster appear) should decrease as $M$ increases. The following monotonicity property on $q_c(M)$ makes this intuition precise.

*Proposition 2.* $q_c(M)$ is a nonincreasing function of $M$, i.e., $q_c(M)\geqslant q_c(M+1),\forall M$.

*Proof.* This is easily proven using sample path arguments. Given a site-occupation probability $q$ for each of $M$ layers, the addition of the $(M+1)$-st layer with the same site-occupation probability can only increase the number of connected sites. Consequently, if a spanning cluster appears in the network with site-occupation probability $q$, then it can only increase in size with the addition of the $(M+1)$-st layer. One practical import of this is that one can limit the search for $q_c(M+1)$ to the interval $(0,q_c(M)]$. ■

## APPENDIX B: AN INTUITIVE ARGUMENT, USING THE COUPON-COLLECTOR PROBLEM, TO SHOW THAT $q_c(M)\leqslant\sqrt{-\ln(1-p_c)}/\sqrt{M}$

In this Appendix, we provide an alternative intuitive argument to show that $\sqrt{-\ln(1-p_c)}/\sqrt{M}$ is an upper bound to $q_c(M)$ for *all* $M\geqslant 1$. In Sec. II, we provided one intuitive argument for the same.

In the classic coupon collector problem, one draws, with replacement, from a box containing $n$ distinct coupons. It is known that $m$ draws, roughly, $n(1-e^{-m/n})$ distinct coupons. Let us say each of the $n=|E|$ bonds of $G$ is a coupon. The expected number of bonds in each layer $G_i$ is $nq^2$, since $q^2$ is the marginal probability of a bond. Therefore, each layer can be regarded as roughly $nq^2$ coupon draws. Hence $M$ layers would be seen as $m=Mnq^2$ coupon draws. $q_c$ is the value of $q$ that corresponds to the number of draws that will fetch just enough distinct coupons (bonds) for the $M$-layer graph to percolate. For standard independent and identically distributed bond percolation, $np_c$ distinct bonds (on an average) would be sufficient for percolation. However, since bond activations are spatially correlated in each layer, $np_c$ coupons will be more than enough for percolation. Hence we get, $np_c\geqslant n[1-e^{-(Mnq_c^2)/n}]$, which translates to $q_c(M)\leqslant\sqrt{-\ln(1-p_c)}/\sqrt{M}$. As the reader would notice, there are several loose ends to the above argument in mapping multilayer percolation to the classic coupon collector problem. To name some: (1) each layer does not draw *exactly* $nq^2$ coupons (it is an expected number); (2) furthermore, the $nq^2$ coupon draws within one layer are done *without replacement* (duplicate bonds can arise only from different layers); (3) a graph with exactly $np_c$ distinct bonds does not guarantee percolation. That number is the average number of bonds at percolation when each bond is drawn independently at random. Finally, (4) the bonds in multilayer percolation are *not* drawn independently at random. Bond activations are spatially correlated. However, it is this last point, as we argue above, that leads to $\sqrt{-\ln(1-p_c)}/\sqrt{M}$ being an *upper* bound to

$q_c(M)$, and the first three points can be dealt with using ideas similar to those used in the proof of Theorem 1.

## APPENDIX C: MULTILAYER RANDOM GRAPH: PROOF THAT $q_c(M)$ IS THE SMALLEST SOLUTION OF $\det(A(q)) = 0$

*Proposition 3.* Assume that $C > 1$. For a random graph with node degree distribution $p_k$, $q_c(M)$ is the smallest solution of

$$\det(\mathbf{A}(q)) = 0 \tag{C1}$$

within the interval $[0,1]$, with $A$ defined in Eq. (3).

*Proof.* Since $\mathbf{A}(0)$ is the identity matrix, $\det(\mathbf{A}(0)) = 1$. On the other hand, it is easy to see that $\det(\mathbf{A}(1)) = 1 - C < 0$ under the assumption that $C > 1$. Therefore, the mapping $q \to \det(\mathbf{A}(q))$ has at least one zero in $[0,1]$. Let $q_0$ be such a zero. For $q$ in the vicinity of $q_0$, $\det(\mathbf{A}(q)) \neq 0$ since $\det(\mathbf{A}(q))$ is a polynomial in the variable $q$. By Cramer's rule,

$$\mu_n(q) = \frac{\det(\mathbf{A}_n(q))}{\det(\mathbf{A}(q))} \tag{C2}$$

for $q$ in the vicinity of $q_0$ with $q \neq q_0$, where $\mathbf{A}_n(q)$ is the matrix formed by replacing the $n$th column of $\mathbf{A}(q)$ by $\mathbf{b}^T$. We claim that there exists at least one $n^\star \in \{1,\ldots,M\}$ such that $\det(\mathbf{A}_{n^\star}(q_0)) \neq 0$. Letting $q \to q_c$, we get from (C2) that $\mu_{n^\star}(q_0) := \lim_{q\to q_0} \mu_{n^\star}(q) = \infty$. Therefore, $\mu_0(q_0) = \infty$ from (2) since $\mu_0(q)$ is expressed as a linear combination of $\mu_1(q),\ldots,\mu_M(q)$ with positive coefficients. This shows that there is an infinite-size spanning cluster (a giant component) when $q = q_0$. Via sample path arguments one can show that there exists an infinite-size spanning cluster for $q > q_c(M)$, where $q_C(M)$ is the smallest zero of $\det(\mathbf{A}(q))$ in $[0,1]$. ■

Numerically, it is easy to verify that $\det(\mathbf{A}(q))$ has a unique zero in $[0,1]$ for all $M \geqslant 1$ as long as $C > 1$. We conjecture that this is always true.

## APPENDIX D: UNIQUENESS OF THE ROOT OF $f_M(q) = 0$, THE ANALYTICAL LOWER BOUND TO $q_c(M)$ FOR THE KAGOME LATTICE

In this Appendix, we provide a proof for the fact that $f_M(q) = 0$ in Eq. (12) has a unique solution in $(0,1)$. Let us take $M \geqslant 1$. We can rewrite $f_M(q)$ as

$$f_M(q) = 3(1-2q^2+q^3)^M - (1-3q^2+2q^3)^M - (1-q^2)^M - Mq^2.$$

The derivative of $f_M(q)$ is $f'_M(q) = 2Mqg_M(q)$ with

$$g_M(q) = \tfrac{3}{2}(3q-4)(1-2q^2+q^3)^{M-1} + 3(1-q)(1-3q^2+2q^3)^{M-1} + (1-q^2)^{M-1} - 1. \tag{D1}$$

We want to show that $g_M(q) \leqslant 0$ for all $q \in [0,1]$ or, equivalently, that the mapping $q \to f_M(q)$ is decreasing in $[0,1]$, which will show that $f_M(q)$ has a unique zero in $[0,1]$ since $f_M(0) = 1$ and $f_M(1) = -M$.

Since

$$(1-2q^2+q^3) - (1-3q^2+2q^3) = q^2(1-q) \geqslant 0$$

for all $q \in [0,1]$, we have that

$$(1-2q^2+q^3)^{M-1} \geqslant (1-3q^2+2q^3)^{M-1} \geqslant 0$$

for all $q \in [0,1]$. So, noting that $3q - 4 < 0$, we have, from (D1),

$$\begin{aligned} g_M(q) &\leqslant \left(\frac{3}{2}(3q-4) + 3(1-q)\right)(1-3q^2+2q^3)^{M-1} + (1-q^2)^{M-1} - 1 \\ &= -3\left(1-\frac{q}{2}\right)(1-3q^2+2q^3)^{M-1} + (1-q^2)^{M-1} - 1 \\ &\leqslant 0. \end{aligned} \tag{D2}$$

The last inequality follows by observing that the first term in the right-hand side of (D2) is always negative and $(1-q^2)^{M-1} - 1 \leqslant 0$ for all $q \in [0,1]$. Hence, the proof that $f_M(q) = 0$ has a unique root in $(0,1)$ is complete.

## APPENDIX E: UNIQUENESS OF THE ROOT OF $g_M(q) = 0$ IN $(0,1]$

It is simple to see why $g_M(q)$ has a unique root in $(0,1]$. We start by taking the derivative of $g_M(q)$ with respect to $q$,

$$\begin{aligned} g'_M(q) &= -2qM(1-q^2)^{M-1} + \frac{M}{C}(1-q)^{M-1} \\ &= \frac{M}{C}(1-q)^{M-1}(1-2qC(1+q)^M). \end{aligned}$$

Let us define $h_M(q) = 1 - 2qC(1+q)^M$, so

$$g'_M(q) = \frac{M}{C}(1-q)^{M-1}h_M(q). \tag{E1}$$

We have

$$\begin{aligned} h'_M(q) &= -2C(1+q)^M - 2qCM(1+q)^{M-1} \\ &= -2C(1+q)^{M-1}(1+qM). \end{aligned}$$

Since $h'_M(q) < 0$ for all $q \in [0,1]$, the mapping $q \to h_M(q)$ is strictly decreasing in $[0,1]$. From $h_M(0) = 1$ and $h_M(1) = 1 - C2^{M+1} < 0$ (since $C > 1$) there exists $q_0$ such that $h_M(q) > 0$ for $q \in [0,q_0)$, $h_M(q_0) = 0$ and $h'_M(q) < 0$ for $q \in (q_0,1]$. Hence, from (E1), we conclude that $g_M(q)$ is increasing in $[0,q_0)$ and decreasing in $(q_0,1]$. Since $g_M(0) = 0$ and $g_M(1) = 1/C - 1 < 0$, which shows that $g_M(q)$ has a unique zero in $(0,1]$.

## APPENDIX F: UNIQUENESS OF THE ROOT OF $f_{SB}(q) = 0$ IN $(0,1)$

In this Appendix, we will prove that $f_{SB}(q)$ has a unique root in $(0,1)$ for any given $p_c$, $q_c$, and $M$. When $M = 1$, $f_{SB}(q)$ has a unique zero in $(0,1)$ at $q = B - A = q_c$. Assume from now on that $M \geqslant 2$. The equation $f_{SB}(q) = 0$ is equivalent to

$$\phi(q) := \frac{1-(1-q)^M + A}{B} = \frac{(1-(1-q)^M)^2}{1-(1-q^2)^M} := \psi(q). \tag{F1}$$

Since $\phi'(q) = M(1-q)^{M-1}/B > 0$ for $q \in (0,1)$ (as $B > 0$) we conclude that the mapping $q \to \phi(q)$ is strictly increasing in $(0,1)$.

Let us now show that the mapping $q \to \psi(q)$ is strictly decreasing $(0,1)$. We find

$$\psi'(q) = 2M[1-(1-q)^M](1-q)^{M-1} \times \frac{[1-(1-q^2)^M - q(1+q)^{M-1}[1-(1-q)^M]]}{(1-(1-q^2)^M)^2} = \frac{2M(1-(1-q)^M)(1-q)^{M-1}}{[1-(1-q^2)^M)^2]}\, v_M(q) \quad \text{(F2)}$$

with $v_M(q) := 1-q(1+q)^{M-1}-(1-q)(1-q^2)^{M-1}$. We have $v_2(q) = -q^3$. Assume that $v_M(q) < 0$ for $q \in (0,1)$ for $M = 2, \ldots, N$ and let us show that $v_{N+1}(q) < 0$ for $q \in (0,1)$.

We have

$$v_{N+1}(q) = v_N(q) - q^2(1+q)^{N-1}[1-(1-q)^N].$$

Since $q^2(1+q)^{N-1}[1-(1-q)^N] > 0$ for $q \in (0,1)$ we conclude from the induction hypothesis that $v_{N+1}(q) < 0$ for $q \in (0,1)$. This proves that $\psi'(q) < 0$ for $q \in (0,1)$, which in turn shows that $\psi(q)$ is strictly decreasing in $(0,1)$.

Because a strictly increasing function and a strictly decreasing function can intersect at most once, we have proved that (F1) has at most one solution in $(0,1)$. It has exactly one solution since $\phi(0) = A/B \leqslant 0$ (as $A \leqslant 0$ and $B > 0$), $\phi(1) = (1+A)/B = 1/p_c > 1$, $\psi(0) = M$ and $\psi(1) = 1$, which shows that $\phi(x)$ and $\psi(x)$ intersect exactly once in $(0,1)$. This completes the proof.

## APPENDIX G: ADAPTATION OF THE NEWMAN-ZIFF ALGORITHM FOR MULTILAYER PERCOLATION

In order to run multilayer simulations on lattices and random graphs, we used an adaptation of the Newman-Ziff technique [17]—an efficient algorithm to simulate site- and/or bond-percolation systems whose runtime is essentially linear (in the number of nodes or sites). This algorithm has been extensively used for numerical analyses of percolating systems and extended to analyzing random graphs [22], continuum percolation on an Eulidean space [36], and interconnected networks [37]. We adapted the Newman-Ziff algorithm (see Appendix G for details) to simulate multilayer percolation for several 2D regular lattices—the square, triangular, kagome, and the family of fully triangulated lattices [27]. Let us first review the basic algorithm.

### 1. The Newman-Ziff algorithm

The underlying idea is based on a union-find algorithm [38]. One chooses a random order in which sites (or bonds) are occupied sequentially, and the algorithm keeps track of all the connected components at each step using a union-find data structure. Each cluster is represented by one *root* member, and every member $i$ is linked to a unique parent $p(i)$ in the same cluster as $i$, except the roots who are their own parents. There are two main functions: `findroot(i)` and `merge(i,j)`. `findroot(i)` follows the links [viz., $p(p(i))\ldots$] from $i$ to the root of its cluster, $r(i)$. Every time a new member $i$ is added to the percolating system, the algorithm iterates through all nearest neighbors of the new member, and for each neighbor $j$ that is occupied, it calls the `merge(i,j)` routine, which uses `findroot(i)` and `findroot(j)` to find $r(i)$ and $r(j)$

**Algorithm 1** MULTILAYERNEWMANZIFF($A, N, M$)

**Require:** The nearest-neighbor matrix $A$ of a graph $G$, and the total number of layers, $M$.

**for** $m = 0$ to $M-1$ **do**
  Initialize: cluster size dummy variable, $C(m) = 0$;
  Generate a random permutation, $\pi_m()$ of $[1, \ldots, n]$;
  **for** $i = 0$ to $N-1$ **do**
    ptr$(m, i)$=EMPTY;
  **end for**
**end for**
**for** $i = 0$ to $N-1$ **do**
  **for** $m = 0$ to $M-1$ **do**
    occupied$(m', \pi_{m'}(i)) = 0$;
    **for** $m' = 0$ to $m$ **do**
      $s_1 = \pi_{m'}(i)$;
      occupied$(m', s-1) = 1$;
      **if** ptr$(m, s_1) \neq$ EMPTY **then**
        $r_1 =$ FINDROOT$(s_1, m)$;
        **if** $-$ptr$(m, r_1) >$ big$(m)$ **then**
          big$(m) = -$ptr$(m, r_1)$;
        **end if**
      **else**
        ptr$(m, s_1) = -1$;
        $r_1 = s_1$;
      **end if**
      **for** $j = 0$ to $d-1$ **do**
        $s_2 = A(s_1, j)$;
        **if** occupied$(m', s_2) = 1$ **then**
          $r_2 =$ FINDROOT$(s_2, m)$;
          **if** $r_2 \neq r_1$ **then**
            **if** ptr$(m, r_1) >$ ptr$(m, r_2)$ **then**
              Increment ptr$(m, r_2)$ by ptr$(m, r_1)$;
              ptr$(m, r_1) = r_2$;
              $r_1 = r_2$;
            **else**
              Increment ptr$(m, r_1)$ by ptr$(m, r_2)$;
              ptr$(m, r_2) = r_1$;
            **end if**
            **if** $-$ptr$(m, r_1) > C(m)$ **then**
              $C(m) = -$ptr$(m, r_1)$;
            **end if**
          **end if**
        **end if**
      **end for**
    **end for**
    ClusterSize$(m, i) = C(m)/N$;
  **end for**
**end for**
**for** $m = 0$ to $M-1$ **do**
  slope$_{\max} = 0$;
  **for** $i = 1$ to $N-1$ **do**
    slope = ClusterSize$(m, i)$-ClusterSize$(m, i-1)$;
    **if** slope $>$ slope$_{\max}$ **then**
      slope$_{\max}$ = slope;
      $q_c(m) = i/N$;
    **end if**
  **end for**
**end for**
**return** multilayer percolation thresholds, $q_c(m)$, $0 \leq m \leq M-1$.
**function** FINDROOT$(i, m)$
  **if** ptr$(m, i) < 0$ **then**
    **return** $i$;
  **end if**
  **return** ptr$(m, i) =$ FINDROOT(ptr$(m, i), m)$;
**end function**

and declares the one whose cluster is larger to be the parent of the other [viz., $p(r(i)) = r(j)$ if $i$'s cluster is smaller than $j$'s], unless of course $r(i) = r(j)$, in which case they are already in the same cluster. The runtime of `findroot(i)` is proportional to the length of the path from $i$ to $r(i)$, which an inductive argument shows can never exceed $\log_2 N$, where $N$ is the system size. Newman-Ziff used a trick called *path compression* to make these paths—averaged over the execution of the algorithm—even smaller. When `findroot(i)` traces its way to $r(i)$, noting that $r(i)$ is the root for each object $j$ along the path from $i$ to $r(i)$, it assigns $p(j) = r(i)$ for all those objects, linking each one directly to the root of the cluster. So next time we call `findroot`, it would work in a single step. With this modification to `findroot()`, the amortized cost of the `findroot` and `merge` operations (cost per operation, averaged over many operations) is *essentially* $O(N)$. To be precise, the amortized cost per step is proportional to the inverse of the Ackermann function $\alpha(N)$, which grows incredibly slowly with $N$ [38].

### 2. Simulation of layered percolation

The first step in setting up the simulation for layered percolation is to create the nearest-neighbor matrix $A$, where $A(i,k) = j$ means node $j$ is the $k$th neighbor of node $i$, $1 \leqslant k \leqslant d(i)$, where $d(i)$ is the degree of node $i$. As an illustration of the construction of the nearest-neighbor matrix, we show in Fig. 10 how we numbered the nodes for the kagome lattice and assigned values to $A(i,k)$ for $0 \leqslant i \leqslant N-1$, $0 \leqslant k \leqslant 3$, for a kagome lattice with $N$ nodes each of degree, $d = 4$.

Algorithm I summarizes the remainder of the algorithm MULTILAYERNEWMANZIFF$(A,N,M)$, which takes as inputs the nearest-neighbor matrix $A$, the number of nodes $N$, and the number of layers $M$ and produces estimates of the multilayer thresholds, $q_c(m)$, $m = 1,\ldots,M$. The algorithm, as written below, accurately estimates the sizes of the largest cluster, ClusterSize$(m,i)$, for an $m$-layer merged lattice as a function of the single-layer site-occupation probability, $q \equiv i/N$. For lattices, the maximum cluster sizes ClusterSize$(m,i)$ have a sharp discontinuity at $q = q_c(m)$ [i.e., $i = i_c \equiv Nq_c(m)$] for an infinite-size lattice [see Fig. 7(a), for instance] for $N$ large enough. Therefore, the $i$ value where the discrete slope of the maximum cluster size [ClusterSize$(m,i)$ − ClusterSize$(m,i-1)$] is maximum gives a pretty good estimate of $i_c(m)$ [hence, that of $q_c(m)$], which suffices for the purposes of this paper. A more accurate way to estimate the threshold $q_c(m)$ involves estimating the *wrapping probabilities*, which are probabilities that a cluster wraps around the lattice boundary conditions, vertically or horizontally or both.


[1] M. Kivelä, A. Arenas, M. Barthelemy, J. P. Gleeson, Y. Moreno, and M. A. Porter, Multilayer networks, J. Complex Netw. **2**, 203 (2014).

[2] S. Boccaletti, G. Bianconi, R. Criado, C. I. del Genio, J. Gómez-Gardeñes, M. Romance, I. Sendiña-Nadal, Z. Wang, and M. Zanin, The structure and dynamics of multilayer networks, Phys. Rep. **544**, 1 (2014).

[3] S. Gómez, A. Díaz-Guilera, J. Gómez-Gardeñes, C. J. Pérez-Vicente, Y. Moreno, and A. Arenas, Diffusion Dynamics on Multiplex Networks, Phys. Rev. Lett. **110**, 028701 (2013).

[4] C. D. Brummitt, K.-M. Lee, and K.-I. Goh, Multiplexity-facilitated cascades in networks, Phys. Rev. E **85**, 045102(R) (2012).

[5] J. Gao, S. V. Buldyrev, H. E. Stanley, Xiaoming Xu, and Shlomo Havlin, Percolation of a general network of networks, Phys. Rev. E **88**, 062816 (2013).

[6] A. Solé-Ribalta, M. De Domenico, N. E. Kouvaris, A. Díaz-Guilera, S. Gómez, and A. Arenas, Spectral properties of the Laplacian of multiplex networks, Phys. Rev. E **88**, 032807 (2013).

[7] D. Cellai, E. López, J. Zhou, J. P. Gleeson, and Ginestra Bianconi, Percolation in multiplex networks with overlap, Phys. Rev. E **88**, 052811 (2013).

[8] V. Nicosia, G. Bianconi, V. Latora, and M. Barthelemy, Growing Multiplex Networks, Phys. Rev. Lett. **111**, 058701 (2013).

[9] V. Marceau, P.-A. Noël, L. Hébert-Dufresne, A. Allard, and L. J. Dubé, Modeling the dynamical interaction between epidemics on overlay networks, Phys. Rev. E **84**, 026105 (2011).

[10] M. De Domenico, A. Solé-Ribalta, E. Cozzo, M. Kivelä, Y. Moreno, M. A. Porter, S. Gómez, and A. Arenas, Mathematical Formulation of Multilayer Networks, Phys. Rev. X **3**, 041022 (2013).

[11] P. Basu, M. Dippel, and R. Sundaram, Multiplex networks: A generative model and algorithmic complexity, in *Proceedings of the IEEE/ACM International Conference on Advances in Social Networks Analysis and Mining (ASONAM'15), Paris, France* (IEEE/ACM, New York, 2015), pp. 456–463.

[12] K.-M. Lee, J. Y. Kim, W.-k. Cho, K.-I. Goh, and I.-M. Kim, Correlated multiplexity and connectivity of multiplex random networks, New J. Phys. **14**, 033027 (2012).

[13] J. Redi and R. Ramanathan, The DARPA WNaN Network Architecture, in *Proceedings of the IEEE Military Communications (MILCOM) Conference, Baltimore* (Elsevier, Amsterdam, 2013), pp. 2258–2263.

[14] F. Buccafurri, V. D. Foti, G. Lax, A. Nocera, and D. Ursino, Bridge analysis in a social internetworking scenario, Inf. Sci. **224**, 1 (2013).

[15] Y. Murase, J. Török, H.-H. Jo, K. Kaski, and J. Kertész, Multilayer weighted social network model, Phys. Rev. E **90**, 052810 (2014).

[16] J. L. Jacobsen, Critical points of Potts and $O(N)$ models from eigenvalue identities in periodic Temperley-Lieb algebras, arXiv:1507.03027 [cond-mat.stat-mech] (2015).

[17] M. E. J. Newman and R. M. Ziff, Efficient Monte Carlo Algorithm and High-Precision Results for Percolation, Phys. Rev. Lett. **85**, 4104 (2000).

[18] M. E. J. Newman, S. H. Strogatz, and D. J. Watts, Random graphs with arbitrary degree distributions and their applications, Phys. Rev. E **64**, 026118 (2001).

[19] M. E. J. Newman, The structure of scientific collaboration networks, Proc. Natl. Acad. Sci. USA **98**, 404 (2000).

[20] D. J. Watts and S. H. Strogatz, Collective dynamics of 'small-world' networks, Nature **393**, 440 (1998).

[21] M. E. J. Newman, Properties of highly clustered networks, Phys. Rev. E **68**, 026121 (2003).
[22] D. S. Callaway, M. E. J. Newman, S. H. Strogatz, and D. J. Watts, Network Robustness and Fragility: Percolation on Random Graphs, Phys. Rev. Lett. **85**, 5468 (2000).
[23] L. A. N. Amaral, A. Scala, M. Barthélémy, and H. E. Stanley, Classes of small-world networks, Proc. Natl. Acad. Sci. USA **97**, 11149 (2000).
[24] M. E. J. Newman, Coauthorship networks and patterns of scientific collaboration, Proc. Natl. Acad. Sci. USA **101**, 5200 (2004).
[25] M. Faloutsos, P. Faloutsos, and C. Faloutsos, On power-law relationships of the Internet topology, Comput. Commun. Rev. **29**, 251 (1999).
[26] http://en.wikipedia.org/wiki/Percolation_threshold.
[27] J. C. Wierman, On the range of bond percolation thresholds for fully triangulated graphs, J. Phys. A: Math. Gen. **35**, 959 (2002).
[28] C. R. Scullard, Exact site percolation thresholds using a site-to-bond transformation and the star-triangle transformation, Phys. Rev. E **73**, 016107 (2006); R. M. Ziff and C. R. Scullard, Exact bond percolation thresholds in two dimensions, J. Phys. A: Math. Gen. **39**, 15083 (2006); R. M. Ziff, Generalized cell–dual-cell transformation and exact thresholds for percolation, Phys. Rev. E **73**, 016134 (2006).
[29] D. P. Kozlenko, A. F. Kusmartseva, E. V. Lukin, D. A. Keen, W. G. Marshall, M. A. de Vries, and K. V. Kamenev, From Quantum Disorder to Magnetic Order in an $s = 1/2$ Kagome Lattice: A Structural and Magnetic Study of Herbertsmithite at High Pressure, Phys. Rev. Lett. **108**, 187207 (2012).
[30] W.-S. Wang, Z.-Z. Li, Y.-Y. Xiang, and Q.-H. Wang, Competing electronic orders on kagome lattices at van Hove filling, Phys. Rev. B **87**, 115135 (2013).
[31] S. C. van der Marck, Percolation thresholds and universal formulas, Phys. Rev. E **55**, 1514 (1997).
[32] D. Achlioptas, R. M. D'Souza, and J. Spencer, Explosive Percolation in Random Networks, Science **323**, 1453 (2009).
[33] J. M. Hammersley, A generalization of McDiarmid's theorem for mixed Bernoulli percolation, Math. Proc. Cambr. Philos. Soc. **88**, 167 (1980).
[34] M. Yanuka and R. Englman, Bond-site percolation: Empirical representation of critical probabilities, J. Phys. A: Math. Gen. **23**, L339 (1990).
[35] Y. Y. Tarasevich and S. C. van der Marck, An investigation of site-bond percolation on many lattices, Int. J. Mod. Phys. C **10**, 1193 (1999).
[36] S. Mertens and C. Moore, Continuum percolation thresholds in two dimensions, Phys. Rev. E **86**, 061109 (2012).
[37] K. J. Schrenk, N. A. M. Araujo, and H. J. Herrmann, Stacked triangular lattice: Percolation properties, Phys. Rev. E **87**, 032123 (2013).
[38] R. E. Tarjan, Efficiency of a good but not linear set union algorithm, J. Assoc. Comput. Mach. **22**, 215 (1975).